BRITISH GEOLOGICAL SURVEY

Natural Environment Research Council

TECHNICAL REPORT WN/92/14

TWO-DIMENSIONAL INVERSION OF THE THORNHILL MT SURVEY DATA

WN/92/14

David Beamish

Bibliographic reference

Beamish, D., Two-dimensional inversion of the Thornhill MT survey data, British Geological Survey, Technical Report WN/92/14.

INTRODUCTION

This report describes the modelling of MagnetoTelluric (MT) survey data carried out in 1992 as part of the Southern Upland mapping programme. The 8-site survey, along a 19 km NW-SE profile was centred on the Thornhill Carboniferous/Permian 'outlier' basin (Figures 1 and 2). The purpose of the survey is to investigate the possibility of 'locally' detecting concealed tectonographic structure by virtue of its (possible) resistivity expression.

The present report provides detailed information on the modelling (inversion) of the survey data. A previous, companion report (Beamish 1992) provided information on the survey and data obtained. The previous report discussed data penetration depths, the lack of evidence for static distortion effects and geoelectric strike azimuths. Although the data characteristics are clearly two-dimensional (2D), the previous report discussed 1D modelling of the higher frequency data to provide simple estimates of the resistivity structure of the Thornhill basin.

The most straightforward interpretation of the near-surface resistivity cross-section across the basin is that the Permian sandstones, with a uniform (vertically averaged) resistivity of 40 ohm.m, extend to a depth of 200 metres in the central part of the basin. This estimate of thickness is in keeping with the modelling of gravity data in the area (Rollin 1991). No significant resistivity contrast appears to exist between the Carboniferous and the underlying lower Paleozoic material. Shallow crustal resistivities for both Ordovician and Silurian formations were estimated as 500 to 600 ohm.m. The cross-section revealed an expected thinning of the Permian towards the SE margin of the basin but an unexpected thickening towards the NW margin.

The main part of this report is concerned with data modelling using regularised 2D inversion techniques. Without such techniques it is arguable whether the complex 2D effects observed across the Thornhill basin could be adequately modelled. The methods reveal that a major conductive feature with a significant dip to the SE underlies the basin and a second, less substantial and near-vertical feature is associated with the basin margin.

DATA DESCRIPTION

The survey and the data obtained were described in detail by Beamish (1992). Site details are here provided in Table 1 and the 8-site profile is shown, in relation to the solid geology in the vicinity of the Thornhill basin, in Figure 1. In order to develop a coordinate system for 2 modelling of the data along profile, an origin of 278, 608 was chosen (Fig. 1). Distances

along the profile in relation to the zero origin are shown in Figure 2.

The smoothed sounding data in the XY-component (N-S direction) at all 8 sites are shown overlaid in two groups in Figure 3, the corresponding YX-component (E-W direction) data are shown in Figure 4. With reference to Figure 1, it should be noted that sites 401, 406 and 408 lie outside the margins of the basin and the soundings at these sites are indicated by continuous lines. Soundings within the basin are indicated by symbols. In Figures 3 and 4 the transition from the southern-most, non-basin site (401) to sites within the basin is demonstrated in the upper 2 decades (100 to 1 Hz) of the soundings. The lowest values of apparent resistivity are recorded at site 405 in both the XY and YX-components. The upper frequency values of resistivity revert to high values at sites 406 and 408 to the NW of the basin.

Overall the sounding data characteristics displayed in Figures 3 and 4 form a spatially complex 'set' across which a number of two-dimensional (2D) contributions are evident and which require assessment by 2D modelling. According to the assessment by Beamish (1992) the data display no evidence for persistent (frequency-independent) static effects but rather display strong 2D behaviour. In terms of dimensional characteristics (Beamish 1992), the high frequency data display 1D/2D characteristics with the 2D contribution increasing with decreasing frequency (increasing penetration depth). An exception to this general behaviour is observed at site 401 which displays more 3D character particularly at low frequencies.

GEOELECTRIC STRIKE AZIMUTHS.

The general behaviour of the geoelectric strike azimuths was discussed by Beamish (1992). In order to assess and model the data within a 2D framework the data need to be rotated to a set of principal azimuths. In a strictly 2D (and no noise) situation the principal azimuths would be identical at all sites and all frequencies, with the possibility of 90 degree rotations occurring across major lateral contrasts. A single principal horizontal azimuth can be obtained from the impedance by analytic or tensor decomposition methods (at each frequency). Figure 5 shows the 2D strike azimuths at low frequencies (0.031 to 0.01 Hz) in plan view. This frequency range represents penetration of the entire crust and the results should relate to the main anisotropy on a crustal scale. The azimuths obtained are largely between +50 and +77 degrees relative to grid north. Figure 6 shows the corresponding results at high frequencies (50 to 10 Hz). The '90 degree' rotations observed indicate that a boundary (lateral resistivity contrast) is traversed between sites 407 and 404 and again between sites 403 and 404.

It is also instructive to examine tensor behaviour by simple graphical rotation. We here examine the behaviour of the off-diagonal element Zyx with tensor rotation though 360 degrees. Figure 7 shows the behaviour of Zyx at low frequencies (0.0189 Hz) at all 8 sites, in two groupings. With the exception of site 401 (3D), the maximum/minimum 90 degree repetition characteristic of a strong 2D contribution can be observed. A reference azimuth at 50 degrees is shown by the dash line. The behaviour of Zyx at 2 Hz is shown in Figure 8 and at 100 Hz in Figure 9. At 2 Hz (Figure 8) tensor behaviour remains 2D with site 401 display partial orthogonal behaviour. At 100 Hz (Figure 9), the tensor behaviour is more 1D (circular rotation) at the majority of sites.

THE ROTATED DATA.

In order to generate an appropriate 2D coordinate system the tensor data were rotated to two orthogonal directions of +50 and +140 degrees. These two directions are consistent with the general attitudes of the principal geoelectric strike azimuths at both high and low frequencies as shown in Figures 5 to 9. Inevitably there are a number of instances where such a 'fixed' rotation introduces a degree of approximation. In the case of site 401 (3D) the degree of approximation is high. At high frequencies at the majority of sites where 1D behaviour is evident, the approximation will be good. At sites and frequencies which display 2D behaviour the degree of the approximation will depend on the general tensor behaviour as indicated in Figures 7 to 9.

The data rotated to +50 degrees will be referred to as TE-mode data (electric field parallel to strike) and the orthogonal data at +150 degrees will be referred to as TM-mode data (magnetic field parallel to strike). The rotated sounding data are shown in Figures 10 (TE-mode) and 11 (TM-mode). In both modes there is a clear grouping at high frequencies at sites within the basin (402, 403, 404, 405) and sites outside (401, 406 and 408). At lower frequencies a complex set of 2D effects is observed. In general terms the TM-mode data (Figure 11) form a more spatially homogenous set of response functions.

2D INVERSION.

The 2D inversion scheme introduced by deGroot-Hedlin and Constable (1990) was used to model the rotated data set. The algorithm is referred to as OCCAM 2D. The approach of OCCAM 2D is to find models fitting the data which are extreme in the sense of having the minimum possible structure. The reasoning behind the approach is that most gridded models

are highly overparameterised in relation to the observed number of data. The OCCAM approach is to conduct a regularised inversion. OCCAM models essentially provide *lower-bounds* on the amount of structure required to fit the observations.

The cross-section for 2D modelling is the 'true' NW-SE profile shown in Figure 1. The origin is taken as the NW corner (278, 608). The regularised OCCAM model was constructed using 26 horizontal blocks, the inner 24 blocks having a dimension of 1 km. The vertical grid was constructed from 24 blocks with the first kilometre containing 4 blocks with a thickness of 250 m. It should be noted that these dimensions imply a relatively crude parameterisation of structure in the first kilometre across the profile. The grid interval is insufficient to adequately 'resolve' the detail of the Thornhill basin at depths of less than 250 m. The essential aim of the initial modelling is to construct a whole crustal cross-section, using the 'average' site spacing of about 2 km or more.

The data rotated to +50 and +140 degrees define the TE- and TM-mode data used by the inversion. In practice a reduced data set is used. The frequency axis of each rotated sounding is resampled at a number of representative frequencies spaced uniformly in log(frequency). For the present data set the 10 frequencies of 100, 35.9, 12.9, 4.64, 1.67, 0.599, 0.2154, 0.0774, 0.0278 and 0.01 Hz were used. In terms of the near-surface model parameterisation, the data at a frequency of 100 Hz cannot be adequately modelled (within the basin) and large errors can be anticipated. The eight sites provide 2 response data (apparent resistivity and phase) in each of the two modes at each frequency. The data set used by the inversion therefore provides 8 x 4 x 10 = 320 degrees of freedom. Site locations in model (profile) coordinates are 408 (2.341 km), 406 (9.70 km), 407 (11.925 km), 405 (13.20 km), 404 (15.55 km), 403 (17.575 km), 402 (18.90 km) and 401 (21.875) km, relative to a zero origin at 278, 608 (see Figure 2).

2D INVERSION RESULTS.

A number of inversion experiments were carried out using the OCCAM 2D algorithm. In each case the initial model consisted of a uniform half space of 500 ohm.m. Since some of the data had error bars which were unrealistic in terms of the 2D approximation (deGroot-Hedlin and Constable 1990), minimum errors were increased to 10% for all data.

The inversion produced a crustal-scale model with an overall misfit of 4.6. This corresponds to fitting all 320 data to within 4.6 standard errors. The resulting model is shown (logarithmic resistivity scale) in Figure 12 (the x4 vertical compression should be noted).

Clearly large scale resistivity contrasts appear confined to the upper 5 km. The middle and lower crust is of highly uniform resistivity with a trend to lower values by the lower crustal interval. There may be some form of modification of the main crustal configuration to the NW (site 408) however the site 408 is rather isolated spatially and therefore 'coverage' is poor. It is suggested that the modelling of the 'main' crustal scale resistivity structure would be better undertaken by combining data from the 1991 Ae Survey (Beamish 1991) with the data here considered. The main interpretation of the Thornhill data concerns the lateral variation in resistivity units observed within the upper 5 kilometres. A more detailed cross-section from the model of Figure 12 is shown in Figure 13. In Figure 13 only the upper 5 km of the section is shown and the vertical exaggeration is x2.

A further feature of OCCAM 2D is its ability to perform a regularised inversion which solves for resistivities and static shifts simultaneously still within a smooth model approach. The philosophy adopted is that there is no reason to model structure at depth if it can be shown that variations in the data may be due to near-surface inhomogeneities. Data inversion using this approach produced a model with a reduced r.m.s. misfit of 3.0 and the model is shown in Figure 14 for comparison with the previous model (Figure 13). Before discussing the near-surface models obtained it is worth considering the misfit levels obtained by the inversion procedure.

Figure 15 shows the observed and modelled apparent resistivity data across the section. Observed data is denoted by continuous lines and the modelled data is denoted by the circle symbols at the 10 discrete frequencies used. The upper plot compares the TE-mode data and the lower plot the TM-mode data. The largest contributions to the misfit occur at low frequencies (0.1 to 0.01 Hz) particularly at sites within the basin (407, 405, 404, 403 and 402). Figure 16 shows the corresponding results for the phase data of the TE-mode data (upper plot) and the TM-mode data (lower plot). At a frequency of 100 Hz, some considerable misfits occur. It is likely that these are caused by the 'inadequate' (too large) scale of the near-surface model parameterisation. Again at low frequencies the largest contributions to the overall misfit occur at sites in the basin. Such low frequency contributions to the misfit indicate that the higher frequency data corresponding to resolution of structure within the upper 5 km, are well-modelled. One interpretation of the increase in misfit at low frequencies is that these are non-2D effects in the observed data caused by the scale of the at-surface basin.

One further useful diagnostic of model fit are the anisotropy ratios defined here as the ratio of TE-mode apparent resistivity to that of the TM-mode. Since misfit errors increase in the formation of a quotient, it is the overall **shape** of the observed/modelled anisotropy ratios

that are of concern. Figure 17 shows the observed data as symbols connected by continuous lines while the corresponding modelled data are the discrete symbols. An anisotropy ratio of unity marks the transition from TE-mode apparent resistivity > TM-mode apparent resistivity to a vice-versa situation. As can be seen in Figure 17, apart from the highest frequency (100 Hz), the overall correspondence between observed and modelled ratios is very good.

We now return to the inversion models shown in Figures 12 and 13. The main features of both models are essentially the same. This means that there is no reason to assume that near-surface static distortion has contributed to the observed data. The essential features of the 2D model are adequately accounted for by the inversion model with an overall r.m.s. misfit of 4.6 shown in Figures 12 and 13.

MODEL INTERPRETATION.

A true scale resistivity cross-section of the upper crust is shown in colour in Figure 18. With reference to the interpretation of the cross-section it should be noted that the model grid has lateral dimensions of only 1 km and vertical dimensions of 250 m within the upper kilometre. Two highly conductive zones with resistivities approaching 1 ohm.m or less are observed. Within the context of lower Paleozoic sequence of 'basement' rocks the two major zones can only be sensibly interpreted in terms of concealed shear zones with constituents which give rise to the enhanced conductivities observed. The major zone of enhanced conductivity underlies the Thornhill basin. The zone possesses a distinct south-easterly dip and is primarily centred between 1.5 and 3 km (see also Figure 12). When interpreting strictly-smooth models it is necessary to allow for the inherent lack of discontinuities which gives rise to finite wavelengths (model blur). The data will also preferentially resolve conductive features across the section. The two relatively resistive features observed across the central portion of the model may, in part, be 'reflections' of the conductive features. No physical interpretation of these zones is attempted.

The true-scale grey scale cross-section shown in Figure 19 is probably more representative of the inherent properties of a smooth inverse solution. The major conductive zone at depth lies beneath the central 'Permian' portion of the Thornhill basin. If the south-easterly dip of the zone is traced to the surface it would outcrop in the vicinity of site 407 on the fault-bounded north-western margin of the basin.

The extent of the outcrop of the Carboniferous (C) and Permian (P) rocks are arrowed in

Figure 19 at the surface. Despite the low resolution of the model at shallow depths, the basin is indicated by an at-surface sequence of relatively conductive blocks (< 100 ohm.m). The thickness portrayed is **necessarily overestimated** by the 2D model. According to Beamish (1992), the Permian sandstones (40 ohm.m) extend to a depth of 200 metres in the central part of the basin, shelve to the SE and thicken to the NW.

A second conductive feature at relatively shallow depth underlies the termination of the basin to the SE. The conductive anomaly is centred on a depth of about 1 km and extends to a depth of only 1.5 km. The feature is highly localised and appears vertical. The zone could be interpreted as either fault-related or a less substantial shear zone in the vicinity of the south-easterly margin of the basin. Further, more detailed, modelling studies would be beneficial. An obvious recommendation is to carry out inversion using the combined MT data sets from Ae and Thornhill surveys with allowance made for a detailed near-surface grid.

REFERENCES

Beamish, D., 1991. A whole crust resistivity cross-section across the Ae Forest, Southern Uplands. *British Geological Survey,* Technical Report, WN/91/25.

Beamish, D., 1992. A magnetotelluric survey across the Thornhill basin, Southern Uplands, *British Geological Survey,* Technical Report, WN/92/11.

deGroot-Hedlin, C. and Constable, S., 1990. Occam's inversion to generate smooth, two-dimensional models from magnetotelluric data, *Geophysics,* **55**, 1613-1624.

Kimbell, G.S., 1991. Magnetic anomalies and the deep structure of the Iapetus convergence zone, *Geophys. J. Int.*, **104**, 687 (Abstract).

Rollin, K.E., 1991. Gravity models of the Upper Palaeozoic deposits near Dumfries. *British Geological Survey,* unpublished manuscript.

FIGURE CAPTIONS

Figure 1. Site locations 401 to 408 (open circles) shown in relation to outcrop geology and main faults. Horizontal hatch : Permian sandstone. Vertical hatch : Carboniferous. Solid infill : Permian basalt.

Figure 2. As per Figure 1 with sites coordinates shown along model (NW-SE) profile with distances in km from a zero origin of 278, 608.

Figure 3. Smoothed sounding data in the XY component at all 8 sites. Sites 401-404 (upper diagram), sites 405-408 (lower diagram).

Figure 4. Smoothed sounding data in the YX component at all 8 sites. Sites 401-404 (upper diagram), sites 405-408 (lower diagram).

Figure 5. Plan view of geoelectric strike azimuths at low frequencies (from .031 to .01 Hz) at all 8 sites. Azimuths relative to grid north.

Figure 6. Plan view of geoelectric strike azimuths at high frequencies (from 50 to 10 Hz) at all 8 sites. Azimuths relative to grid north.

Figure 7. Tensor anisotropy at 0.0189 Hz. Impedance element Zyx rotated through 360 degrees at sites 401-404 (upper) and 405-408 (lower). Reference (heavy-dash) azimuth is 50 degrees.

Figure 8. Tensor anisotropy at 2 Hz. Impedance element Zyx rotated through 360 degrees at sites 401-404 (upper) and 405-408 (lower). Reference (heavy-dash) azimuth is 50 degrees.

Figure 9. Tensor anisotropy at 100 Hz. Impedance element Zyx rotated through 360 degrees at sites 401-404 (upper) and 405-408 (lower). Reference (heavy-dash) azimuth is 50 degrees.

Figure 10. Smoothed rotated sounding data (+50 degrees) defining the TE-mode. Sites 401-404 (upper), sites 405-408 (lower).

Figure 11. Smoothed rotated sounding data (+140 degrees) defining the TM-mode. Sites 401-404 (upper), sites 405-408 (lower).

Figure 12. Whole crust 2D model produced by OCCAM inversion. Vertical compression x 4. R.M.S. misfit of 4.63. Resistivities shown using a logarithmic scale. Boundary crosses denote site locations.

Figure 13. Near-surface 2D model (detail from Fig. 12) produced by OCCAM inversion. Vertical exaggeration x 2. R.M.S. misfit of 4.63. Resistivities shown using a logarithmic scale.

Figure 14. Near-surface 2D model (detail) produced by OCCAM inversion using the static shift option (allowance for possible offsets due to galvanic distortion). Vertical exaggeration x 2. R.M.S. misfit of 3.0. Resistivities shown using a logarithmic scale.

Figure 15. Comparison of observed data (lines with small solid dots) and model response data (open circles) for OCCAM model with r.m.s. misfit of 3.0. Apparent resistivities for the TE-mode (upper) and TM-mode (lower). Scale bars (bottom right) represent 2 decade logarithmic scales.

Figure 16. Comparison of observed data (lines with small solid dots) and model response data (open circles) of OCCAM model with r.m.s. misfit of 3.0. Phase values for the TE-mode (upper) and TM-mode (lower). Scale bars (bottom right) represent 90 degrees.

Figure 17. Comparison of observed (lines with symbols) and model (symbols) anisotropy ratios (ρ<TE>/ρ<TM>). Sites 401-404 (upper), sites 405-408 (lower).

Figure 18. True scale colour plot of 2D OCCAM model (Figure 12 and 13) with r.m.s. misfit 4.63. Resistivities shown using a logarithmic scale.

Figure 19. True scale resistivity cross-section (as per Fig. 18) but defining model blur and significant features resolved by a 'smooth' model. Boundary crosses denote site locations. Arrows denote surface outcrop of Carboniferous (C) and Permian (P).

TABLE 1. THORNHILL MT SURVEY. SITE DETAILS.

The 8 sounding locations which comprise the Thornhill MT survey of 1992 are listed 401-408. The survey comprises a NW-SE traverse with site 401 defining the southern-most site and site 408 defining the northern-most site. Date refers to site occupation. National Grid coordinates and elevations (from 1:25000 O.S. maps) are given in metres.

SITE CODE	DATE	EASTING (m)	NORTHING (m)	ELEVATION (m)
401	21/07/92	292600	592720	175
402	22/07/92	290950	595130	135
403	23/07/92	289780	595800	107
404	24/07/92	289100	597850	180
405	25/07/92	286930	598900	67
407	28/07/92	285600	599350	70
406	26/07/92	284450	601250	212
408	27/07/92	280100	606820	220

Fig.1

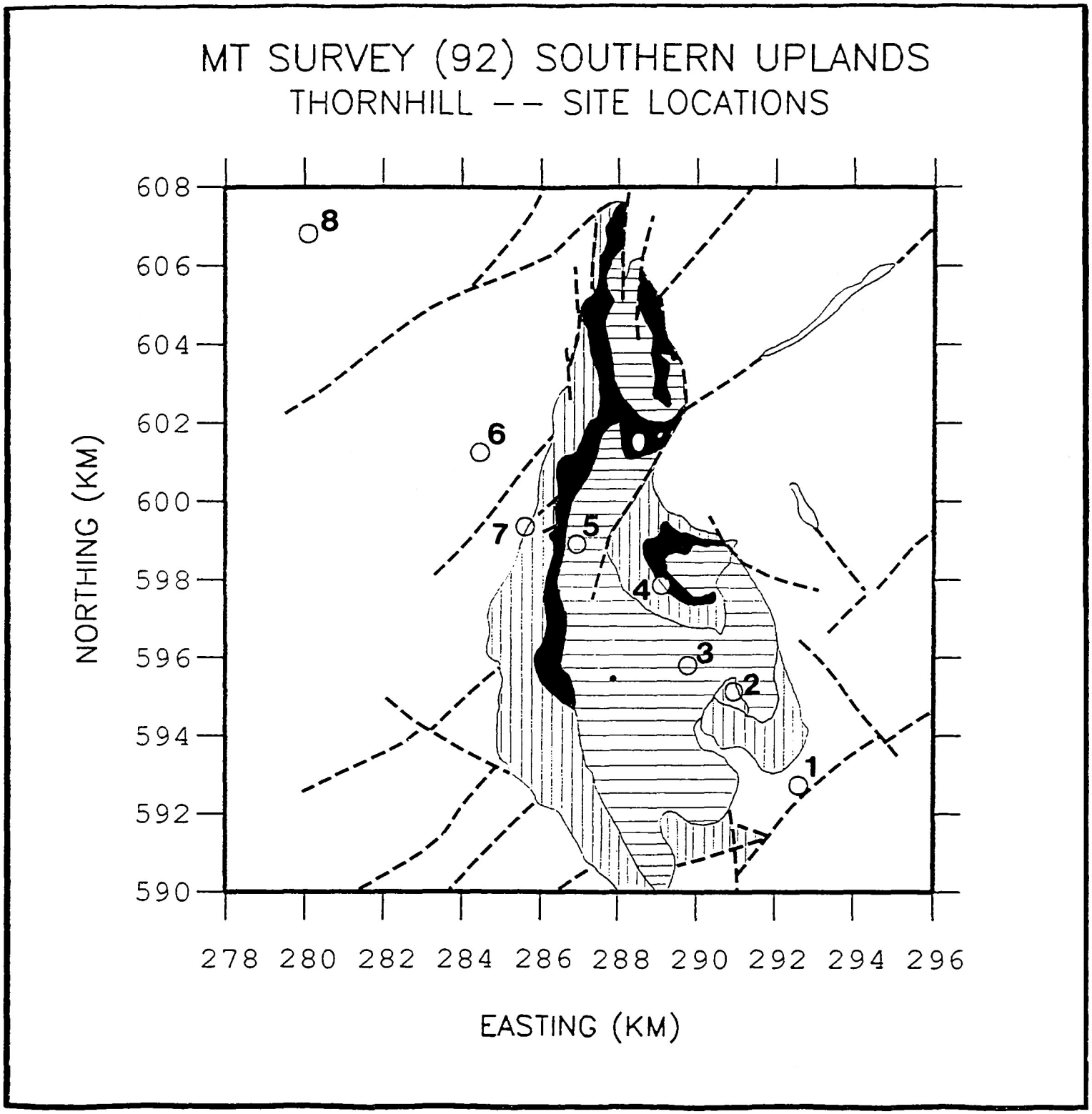
MT SURVEY (92) SOUTHERN UPLANDS
THORNHILL -- SITE LOCATIONS
NORTHING (KM)
608
606
604
602
600
598
596
594
592
590
278 280 282 284 286 288 290 292 294 296
EASTING (KM)
8
6
7
5
4
3
2
1

Fig.2

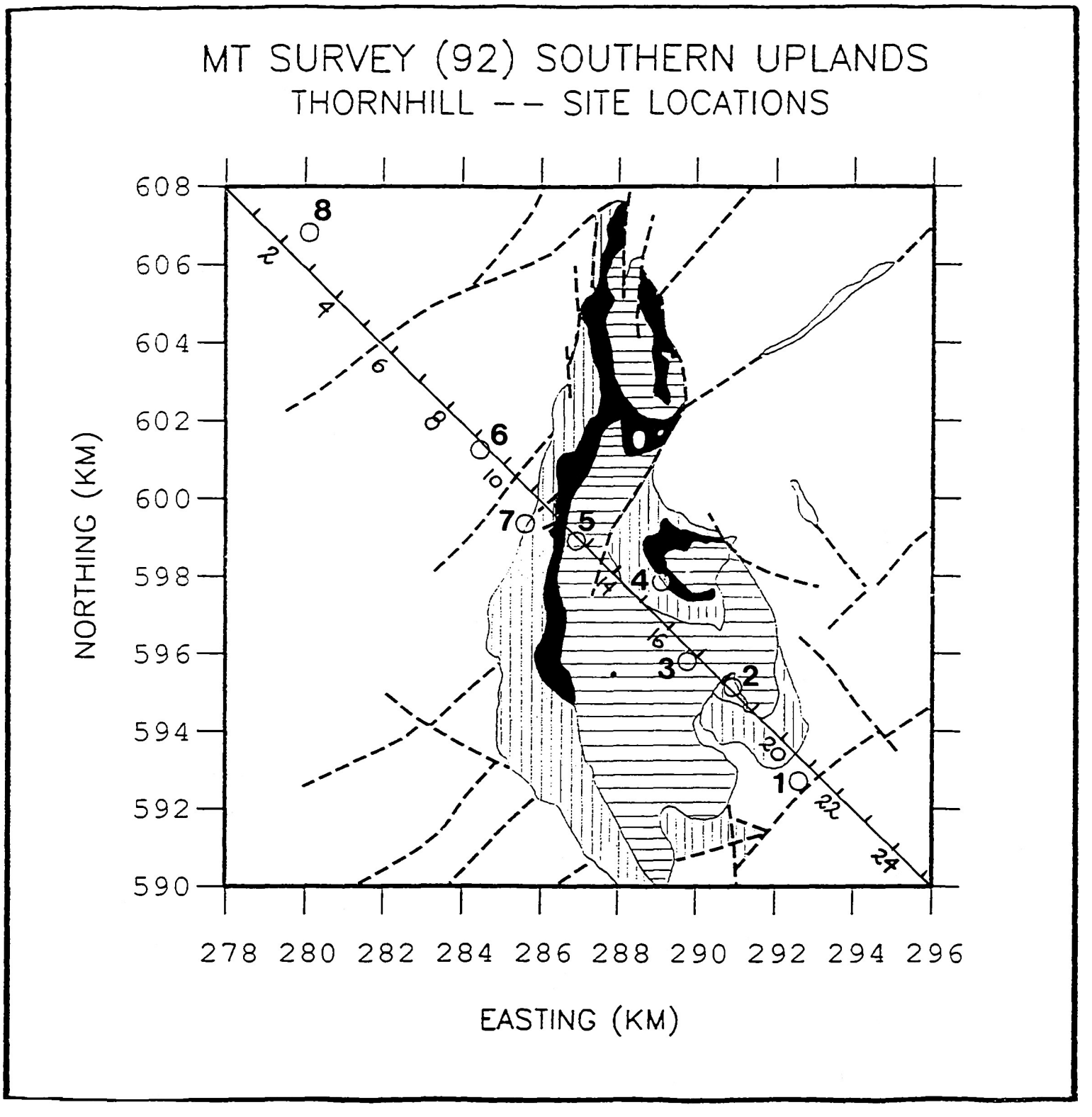
MT SURVEY (92) SOUTHERN UPLANDS
THORNHILL -- SITE LOCATIONS
NORTHING (KM)
608
606
604
602
600
598
596
594
592
590
278 280 282 284 286 288 290 292 294 296
EASTING (KM)
8
6
7
5
4
3
2
1
2
4
6
8
10
12
14
16
18
20
22
24

Fig.3

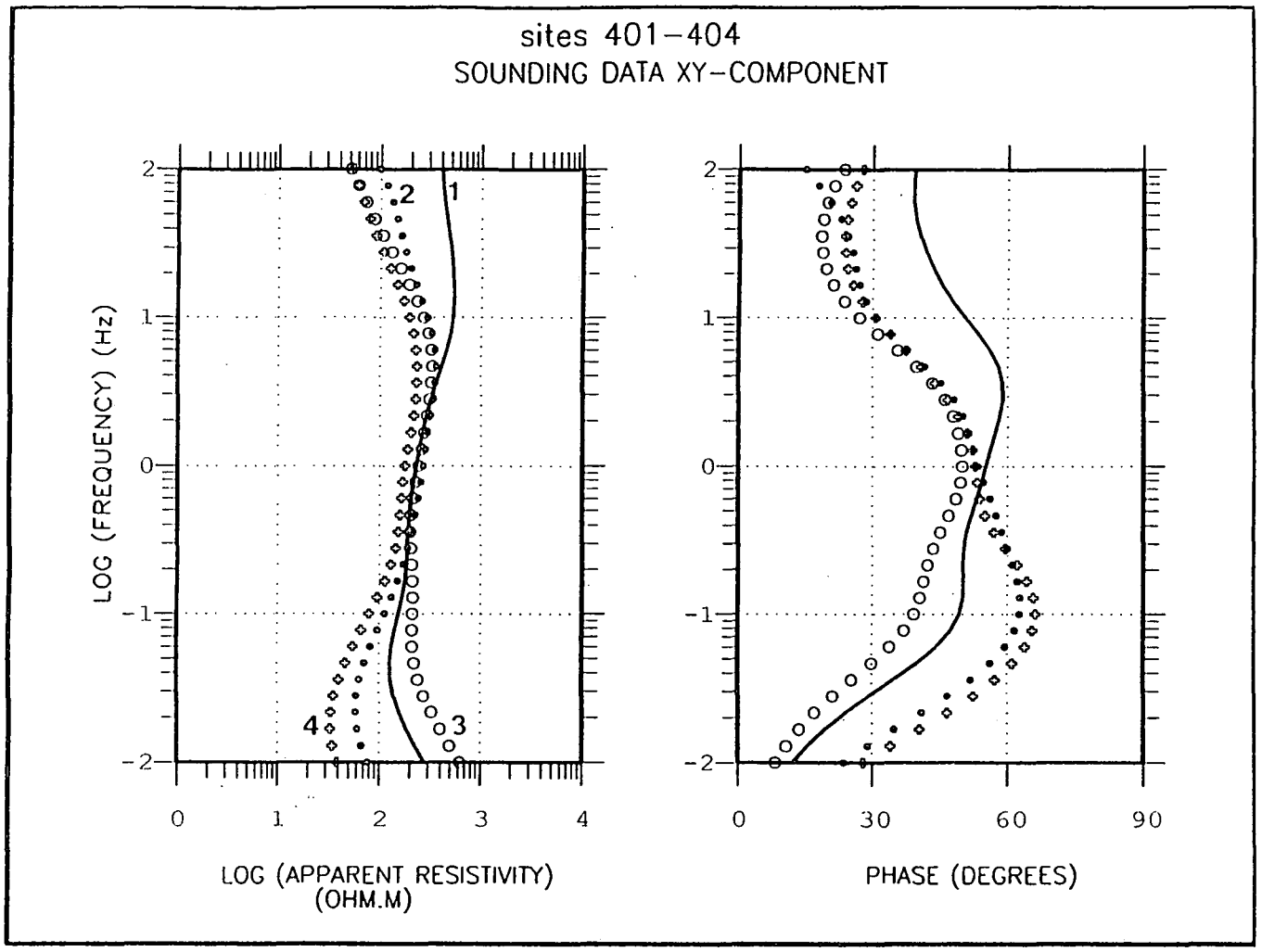
sites 401–404
SOUNDING DATA XY–COMPONENT
LOG (FREQUENCY) (Hz)
2
1
0
-1
-2
1
2
3
4
0
30
60
90
LOG (APPARENT RESISTIVITY)
(OHM.M)
PHASE (DEGREES)

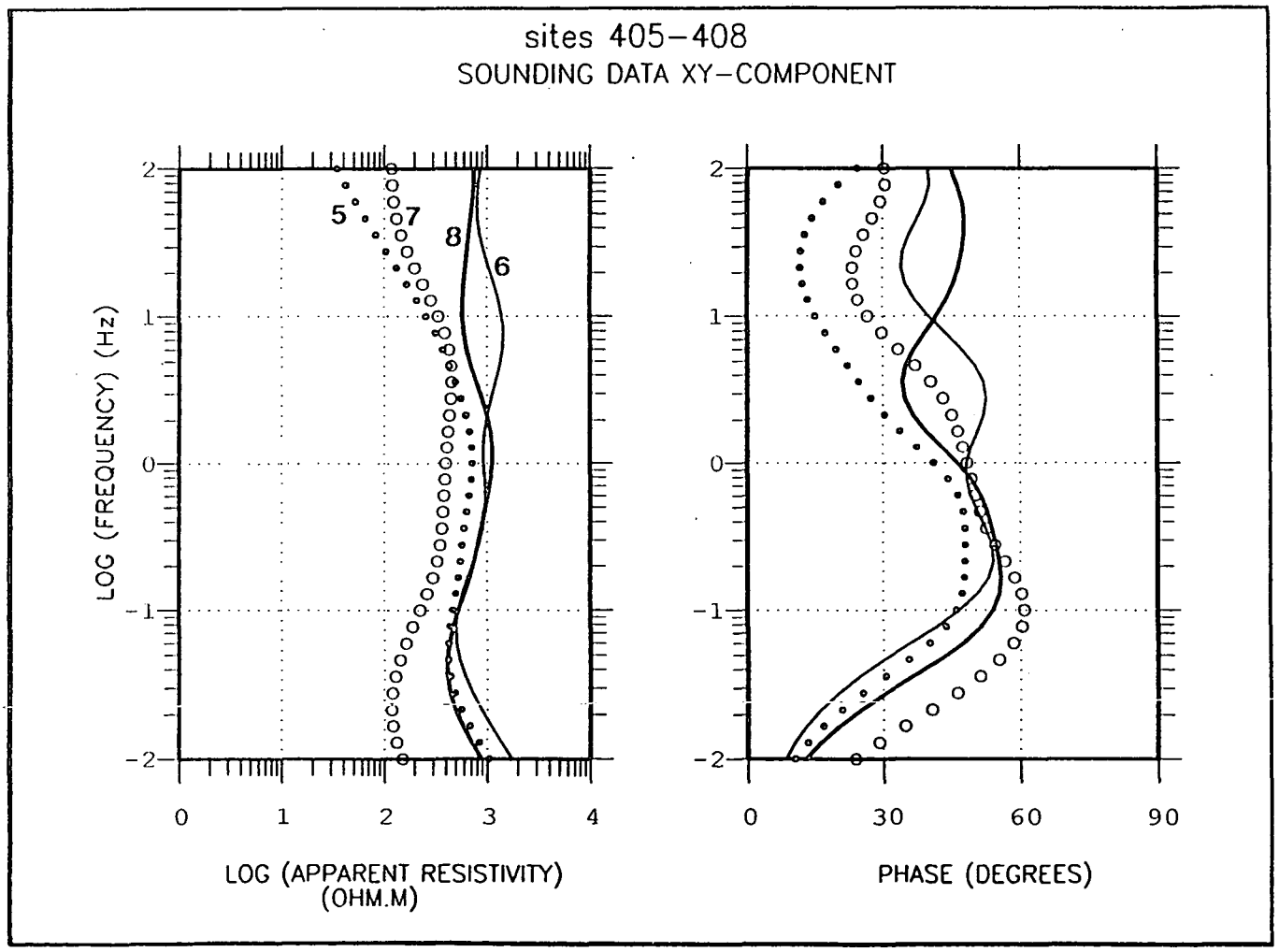
sites 405–408
SOUNDING DATA XY–COMPONENT
LOG (FREQUENCY) (Hz)
2
1
0
-1
-2
5
7
8
6
0
1
2
3
4
0
30
60
90
LOG (APPARENT RESISTIVITY)
(OHM.M)
PHASE (DEGREES)

Fig.4

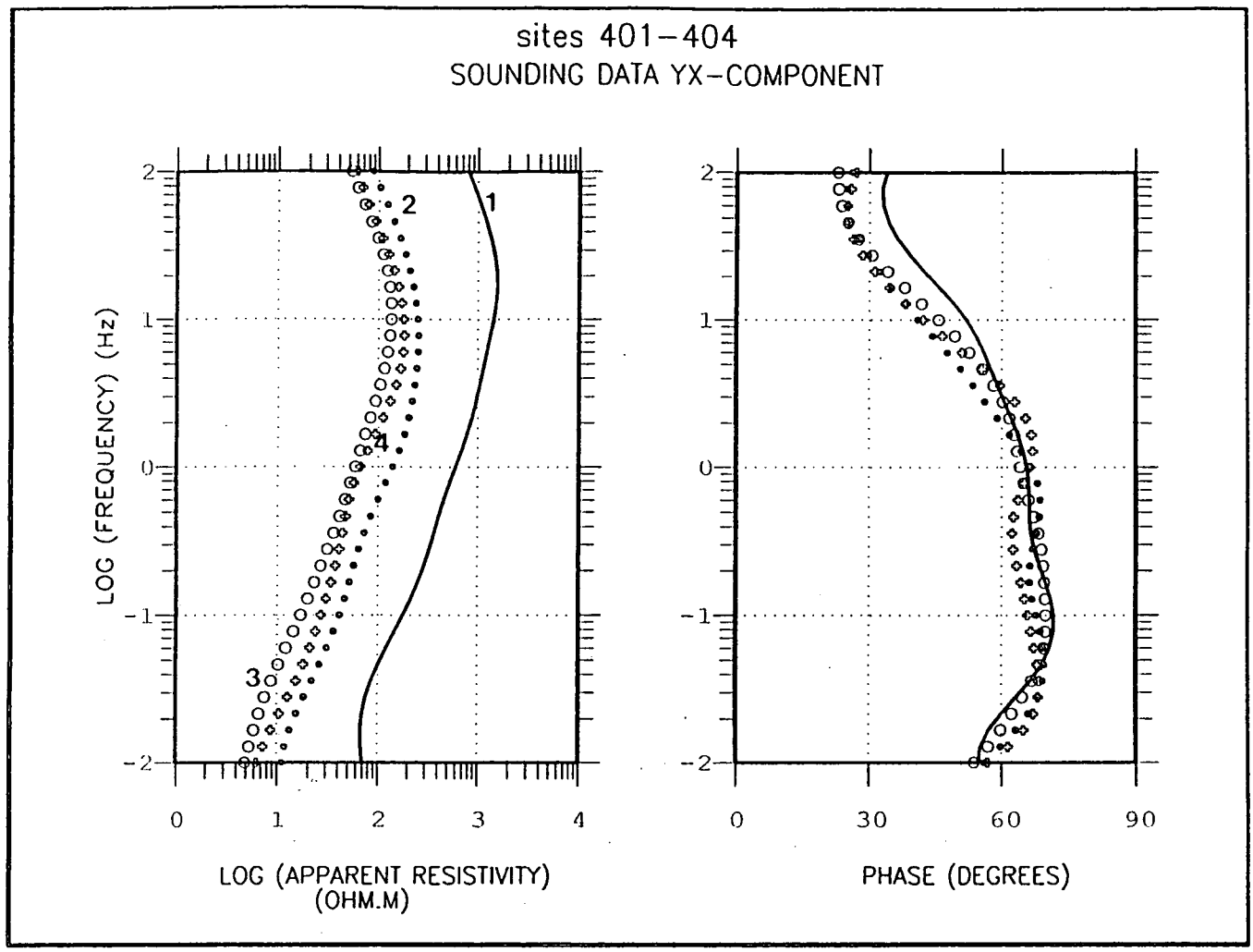
sites 401–404
SOUNDING DATA YX–COMPONENT
LOG (FREQUENCY) (Hz)
2
1
0
-1
-2
1
2
3
4
0
1
2
3
4
LOG (APPARENT RESISTIVITY)
(OHM.M)
0
30
60
90
PHASE (DEGREES)

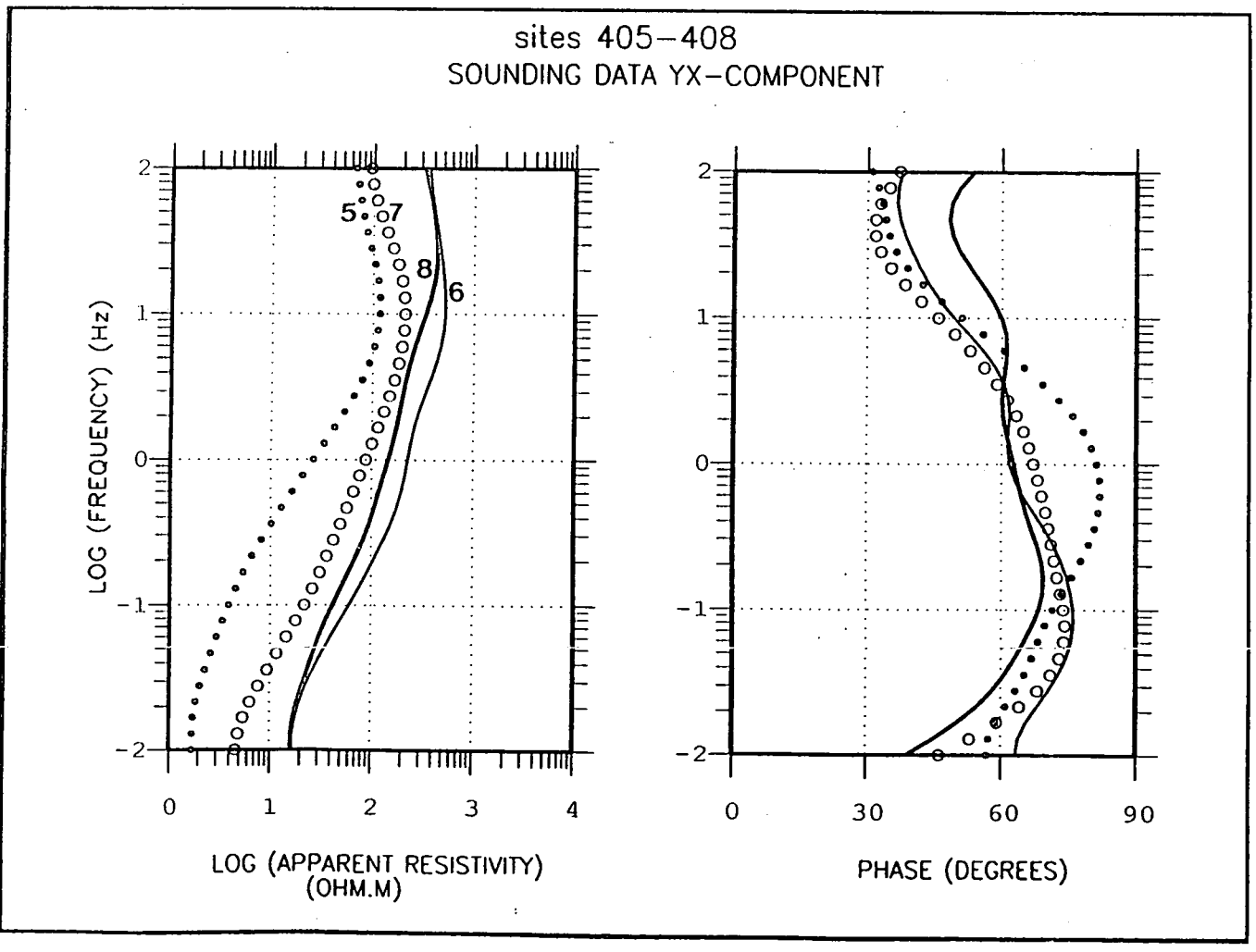
sites 405–408
SOUNDING DATA YX–COMPONENT
LOG (FREQUENCY) (Hz)
2
1
0
-1
-2
5
7
8
6
0
1
2
3
4
LOG (APPARENT RESISTIVITY)
(OHM.M)
0
30
60
90
PHASE (DEGREES)

Fig.5

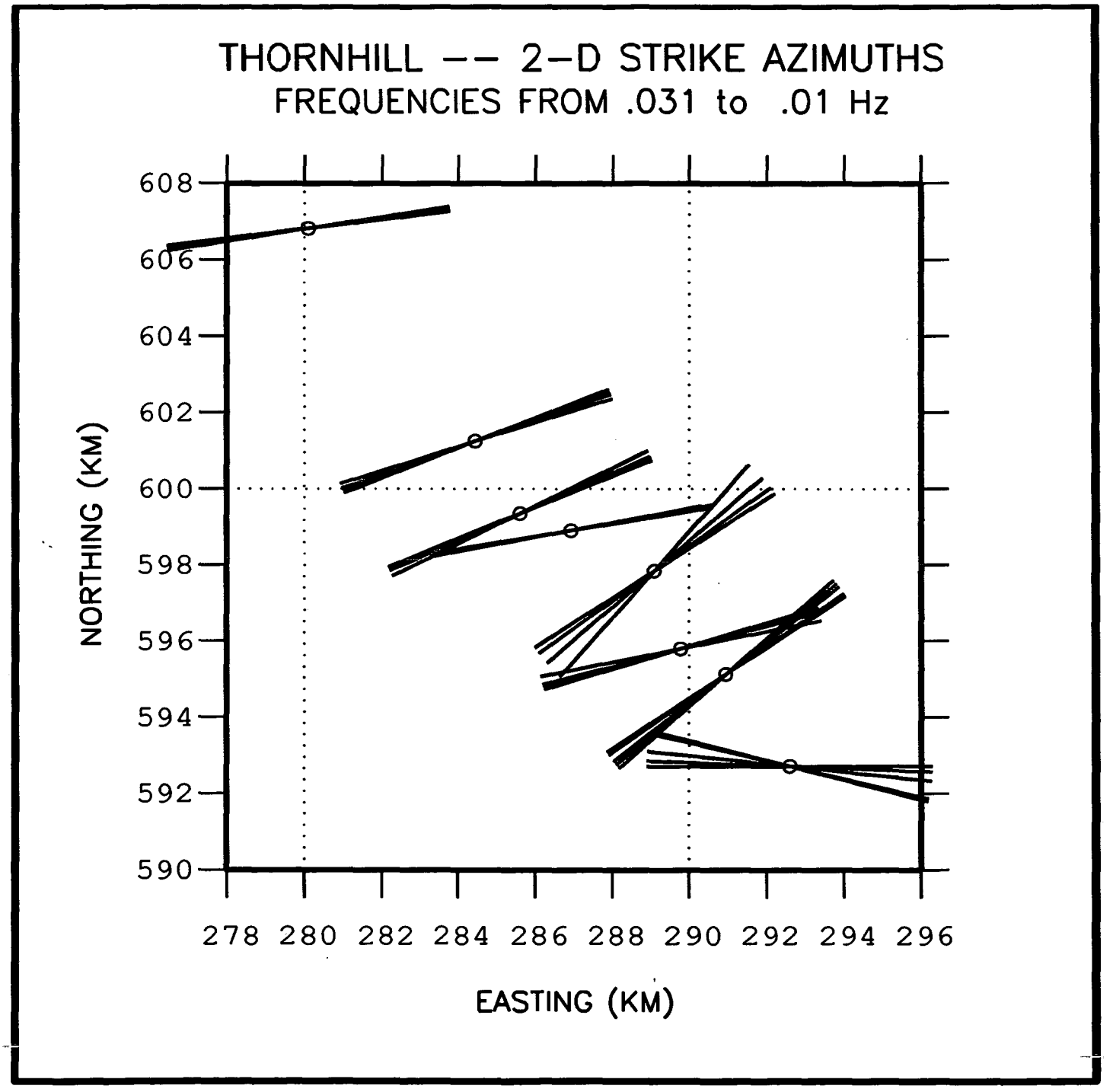
THORNHILL -- 2-D STRIKE AZIMUTHS
FREQUENCIES FROM .031 to .01 Hz
608
606
604
602
600
598
596
594
592
590
NORTHING (KM)
278 280 282 284 286 288 290 292 294 296
EASTING (KM)

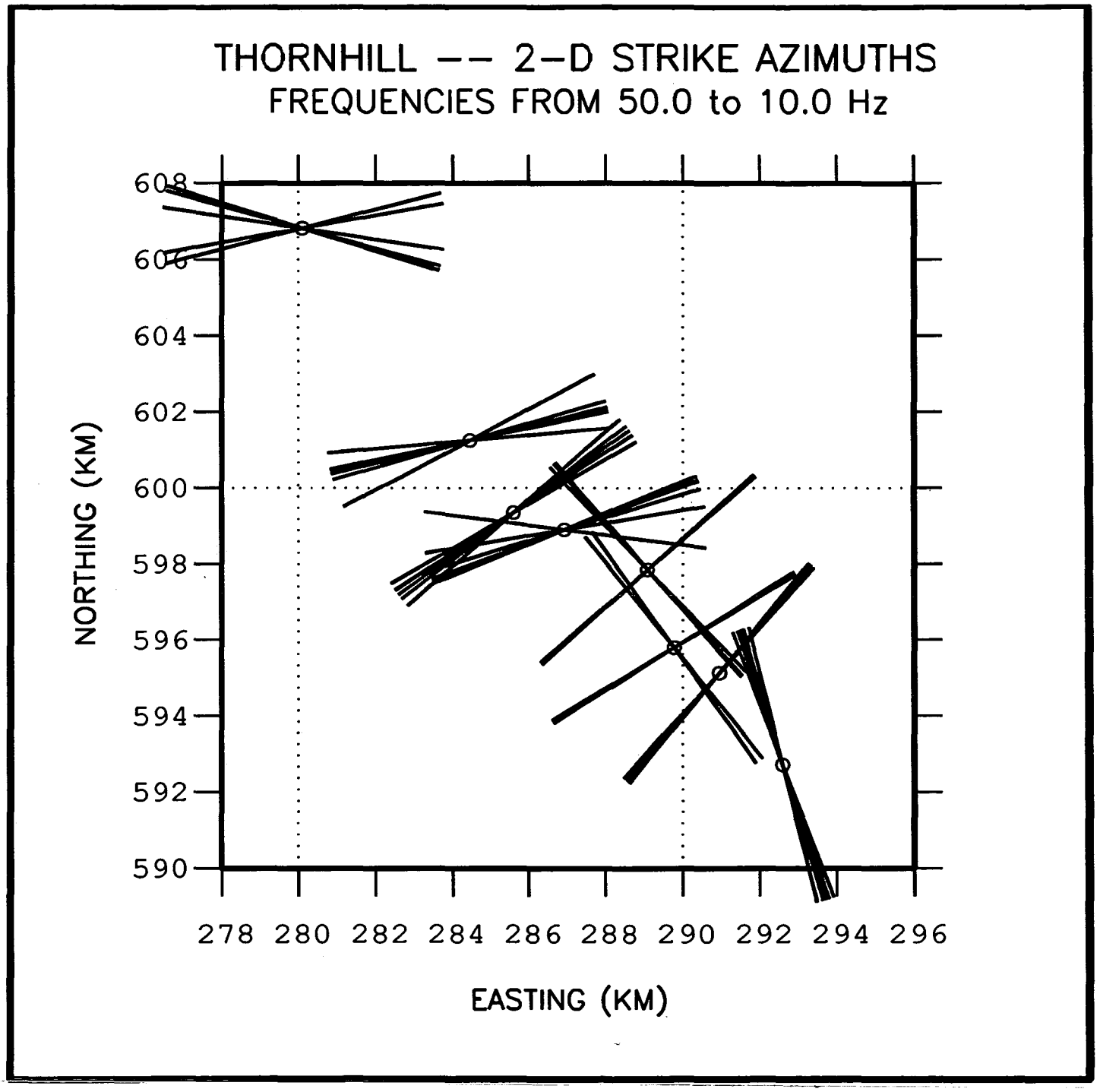
THORNHILL -- 2-D STRIKE AZIMUTHS
FREQUENCIES FROM 50.0 to 10.0 Hz
608
606
604
602
600
598
596
594
592
590
NORTHING (KM)
278 280 282 284 286 288 290 292 294 296
EASTING (KM)

TENSOR ANISOTROPY, sites 401, 402, 403, 404

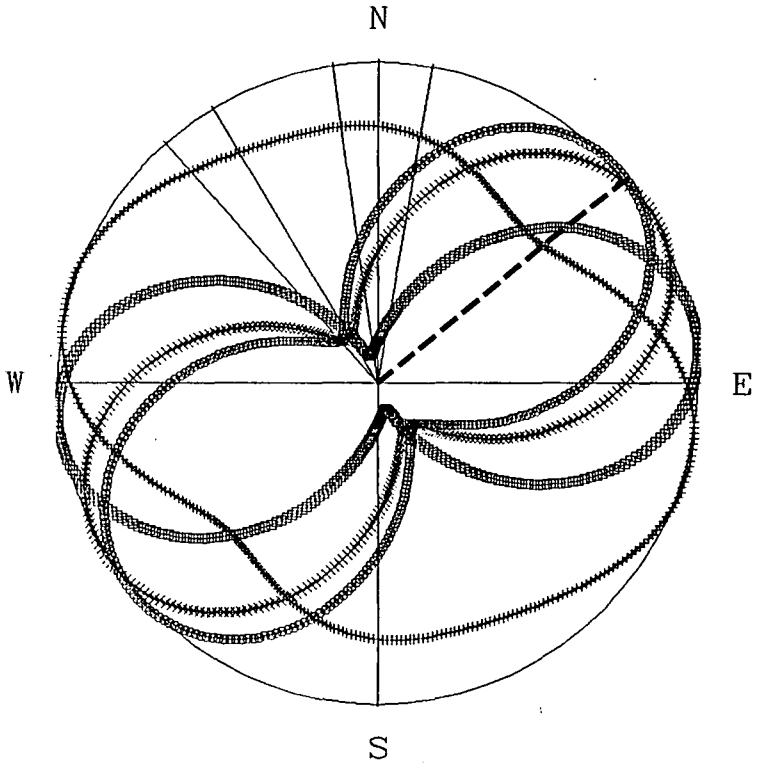

<Zyx> FREQUENCY 0.0189 Hz

TENSOR ANISOTROPY, sites 405, 407, 406, 408

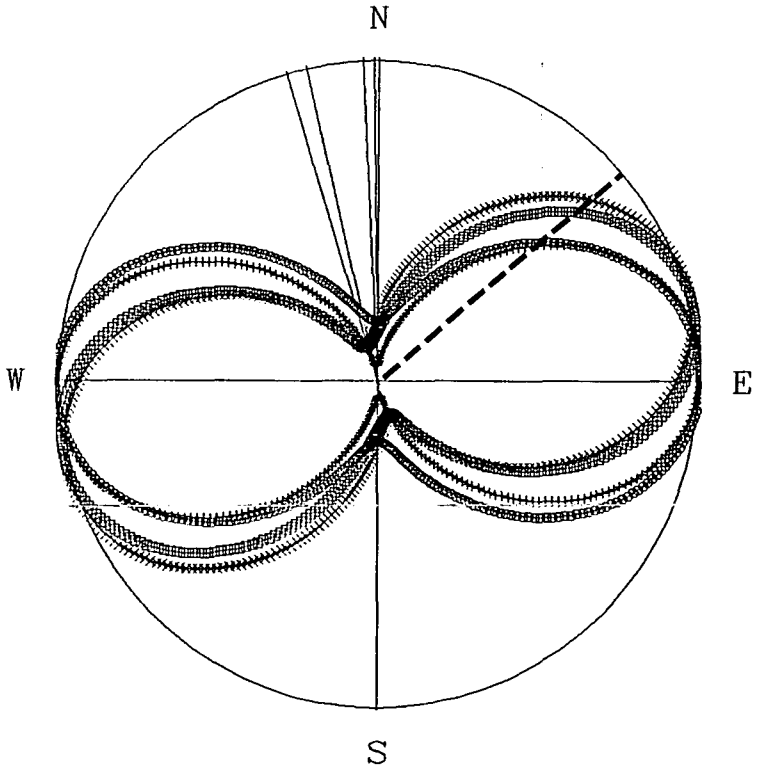

<Zyx> FREQUENCY 0.0189 Hz

TENSOR ANISOTROPY, sites 401, 402, 403, 404

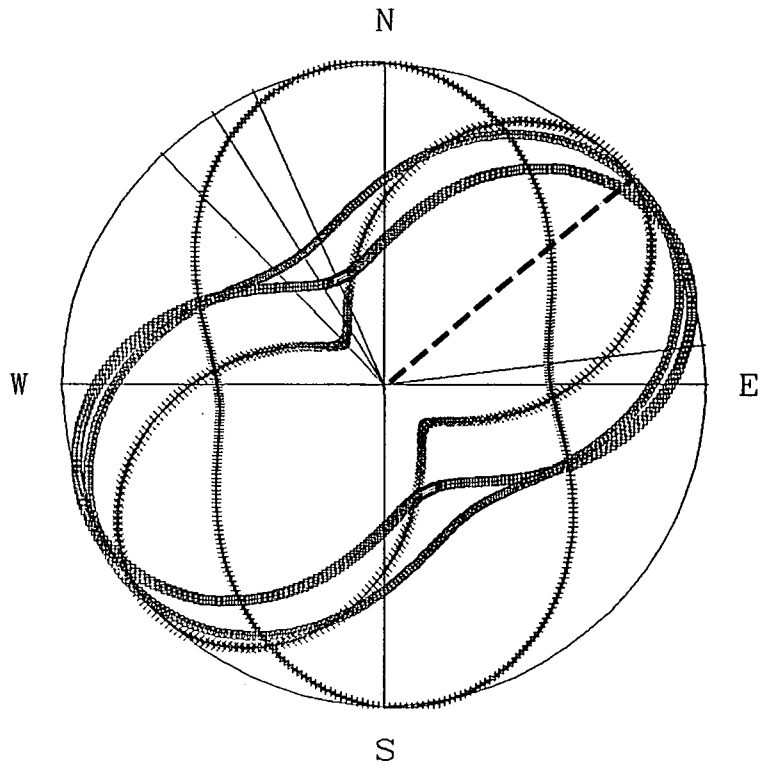

<Zyx> FREQUENCY 2 Hz

TENSOR ANISOTROPY, sites 405, 407, 406, 408

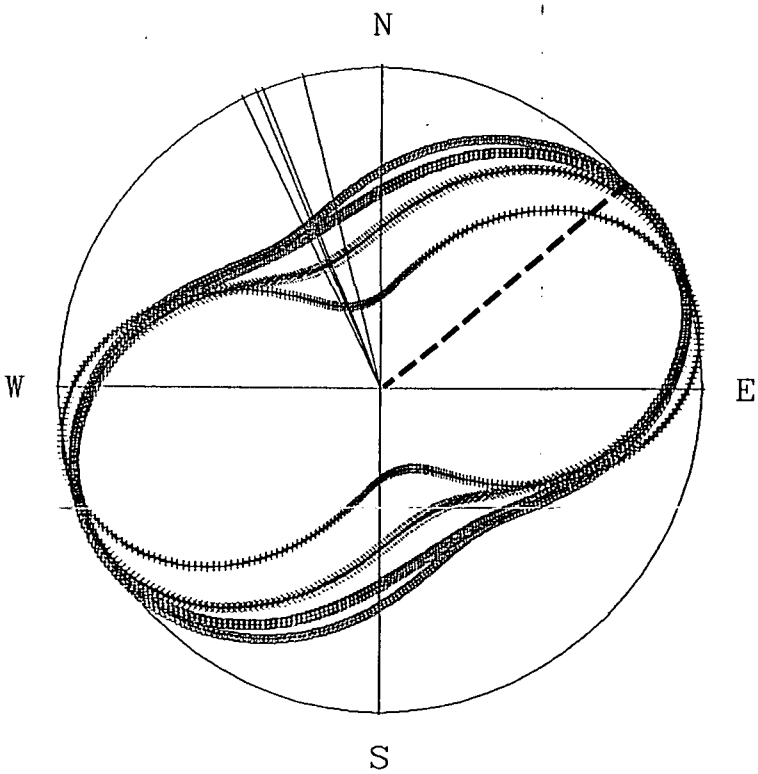

<Zyx> FREQUENCY 2 Hz

TENSOR ANISOTROPY, sites 401, 402, 403, 404

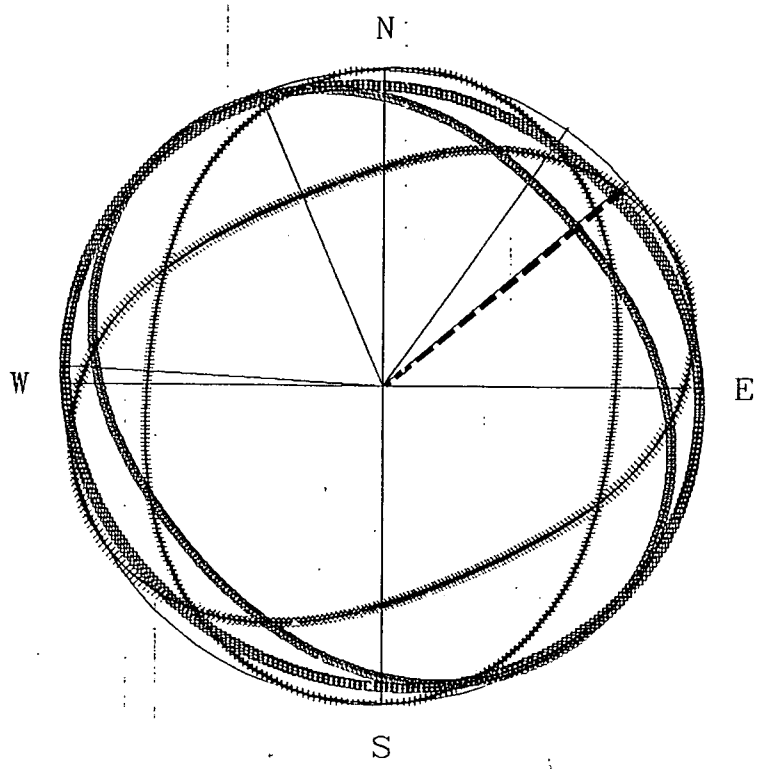

<Zyx> FREQUENCY 100 Hz

TENSOR ANISOTROPY, sites 405, 407, 406, 408

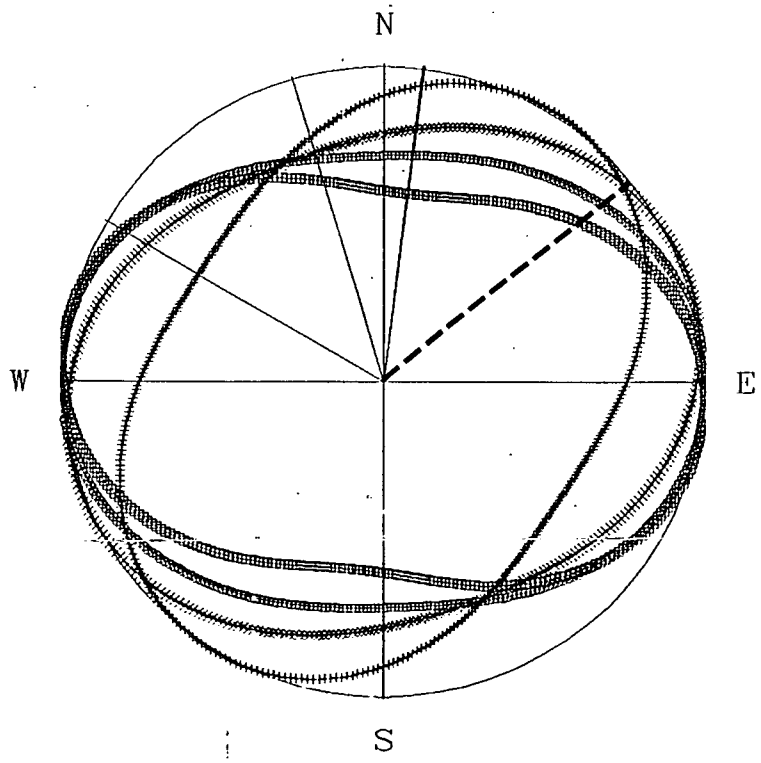

<Zyx> FREQUENCY 100 Hz

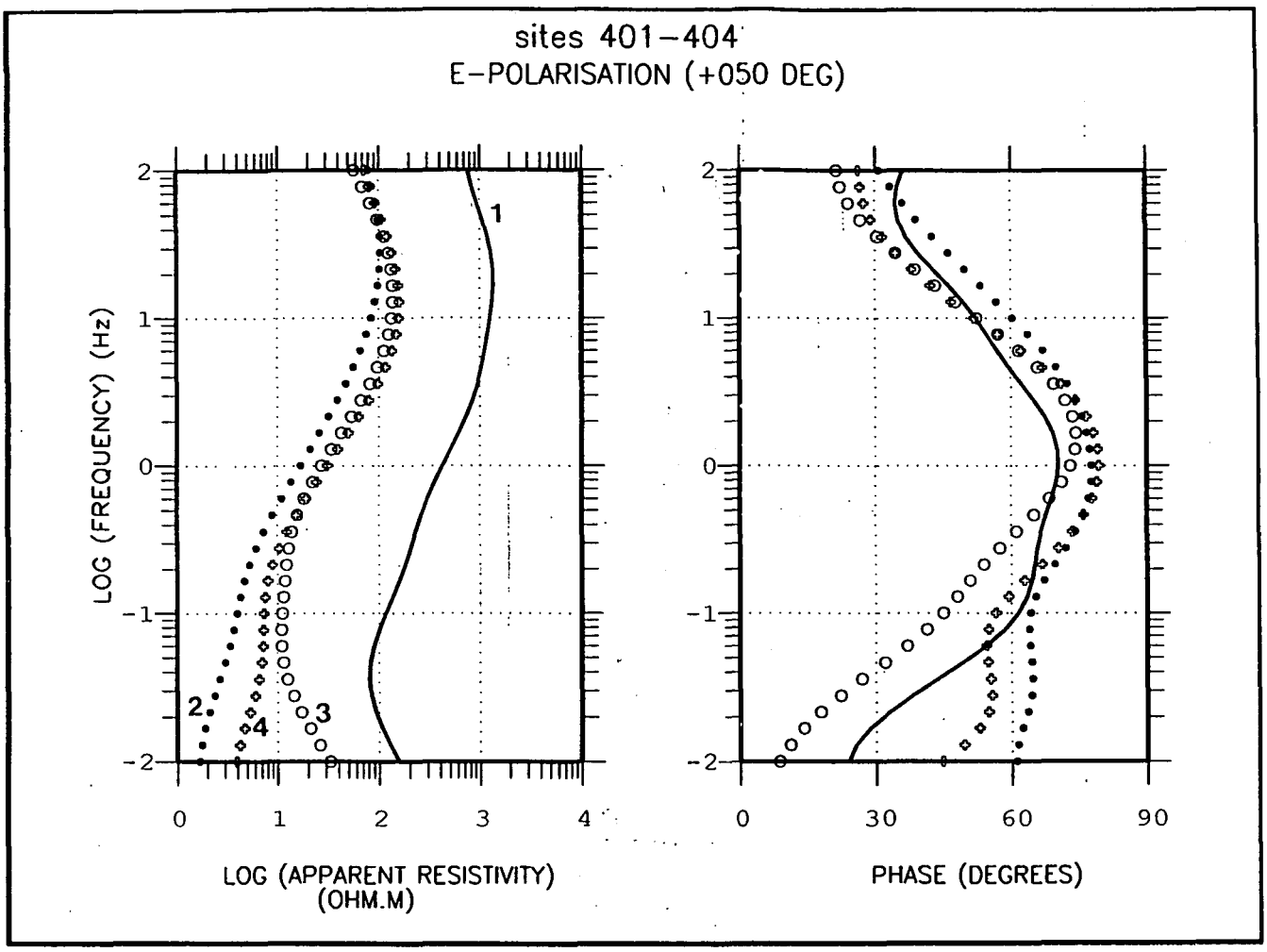
sites 401–404
E–POLARISATION (+050 DEG)
LOG (FREQUENCY) (Hz)
2
1
0
-1
-2
1
2
3
4
0
1
2
3
4
LOG (APPARENT RESISTIVITY)
(OHM.M)
0
30
60
90
PHASE (DEGREES)

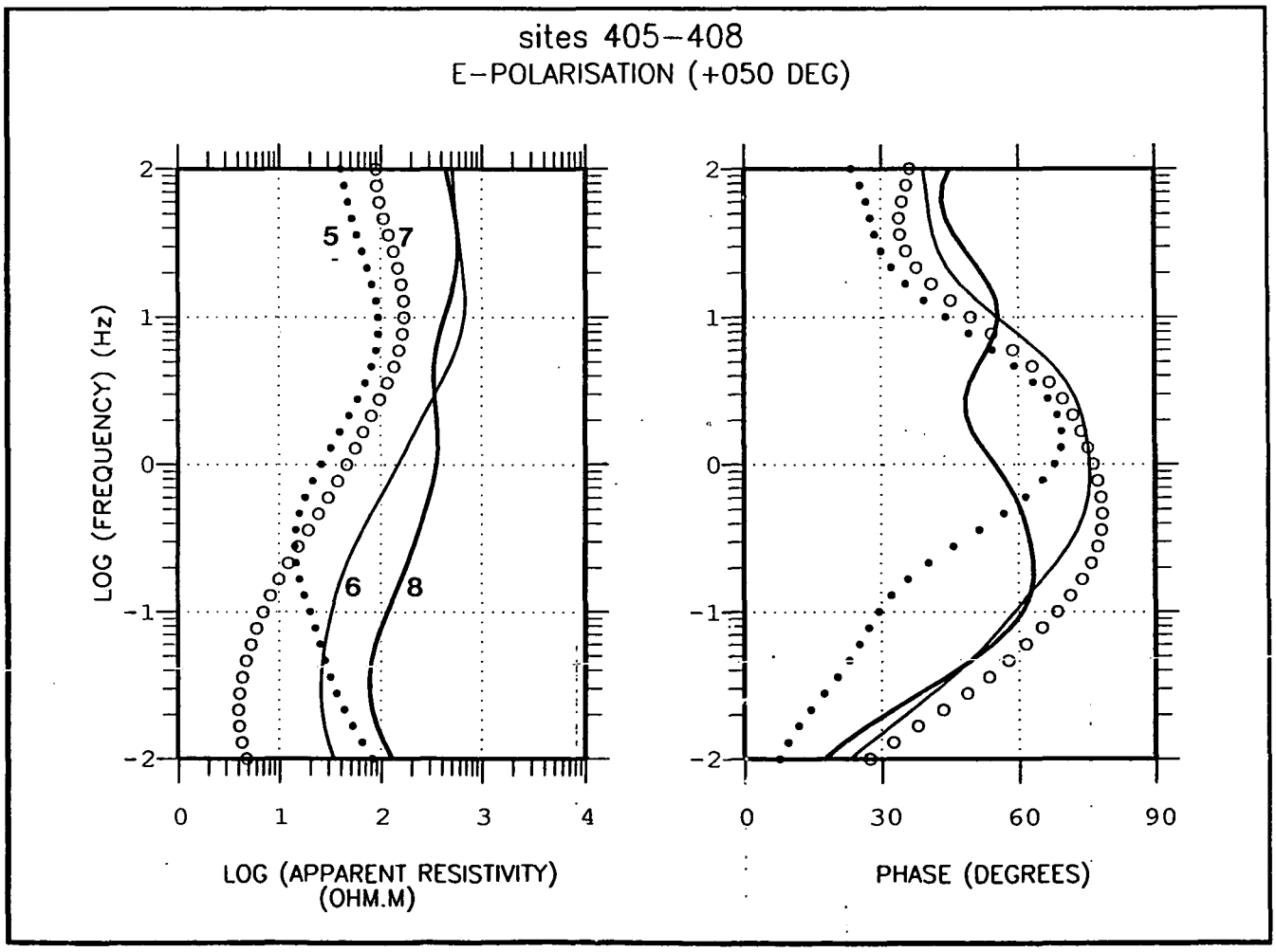
sites 405–408
E–POLARISATION (+050 DEG)
LOG (FREQUENCY) (Hz)
2
1
0
-1
-2
5
7
6
8
0
1
2
3
4
LOG (APPARENT RESISTIVITY)
(OHM.M)
0
30
60
90
PHASE (DEGREES)

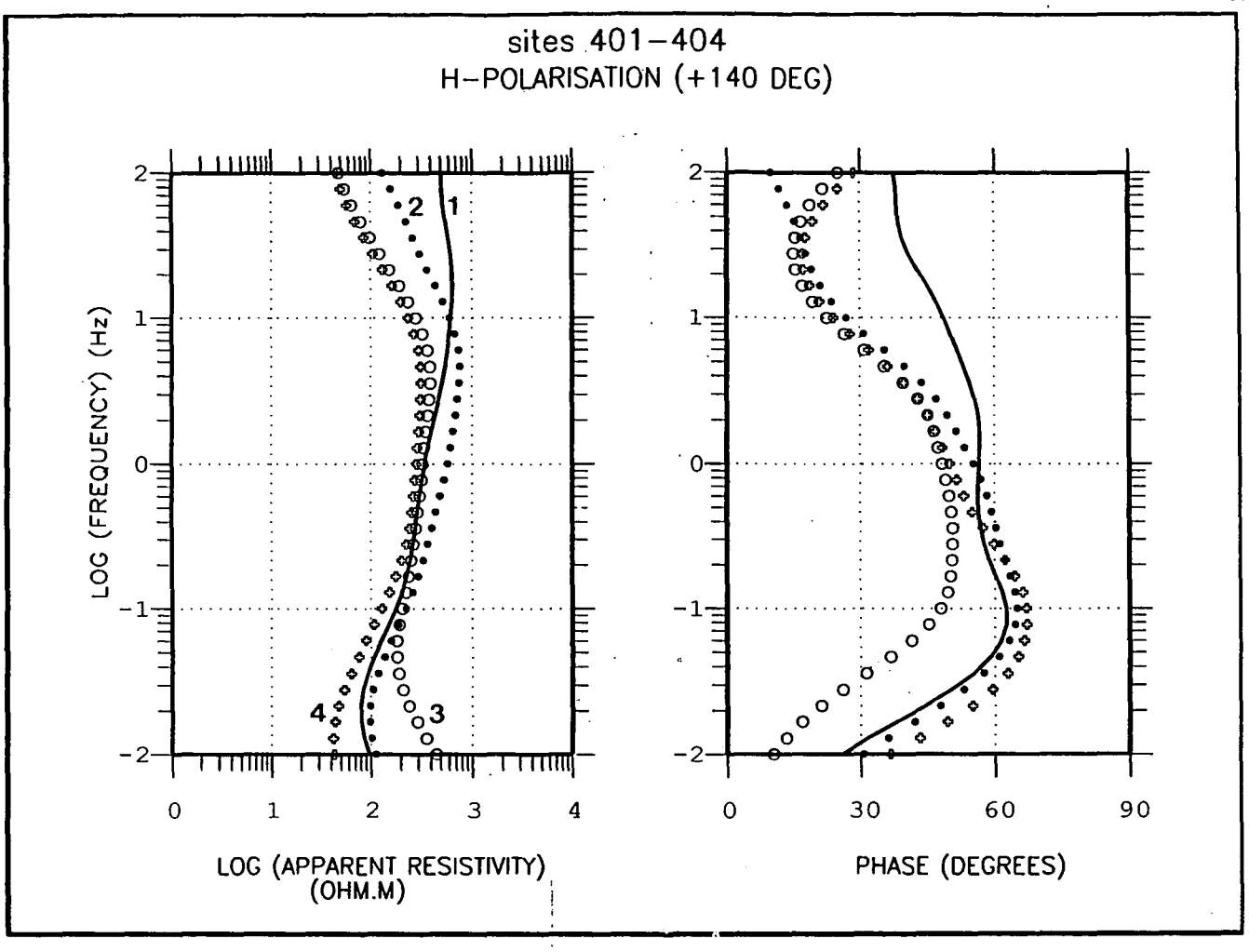
sites 401–404
H–POLARISATION (+140 DEG)
LOG (FREQUENCY) (Hz)
2
1
4
3
LOG (APPARENT RESISTIVITY)
(OHM.M)
PHASE (DEGREES)

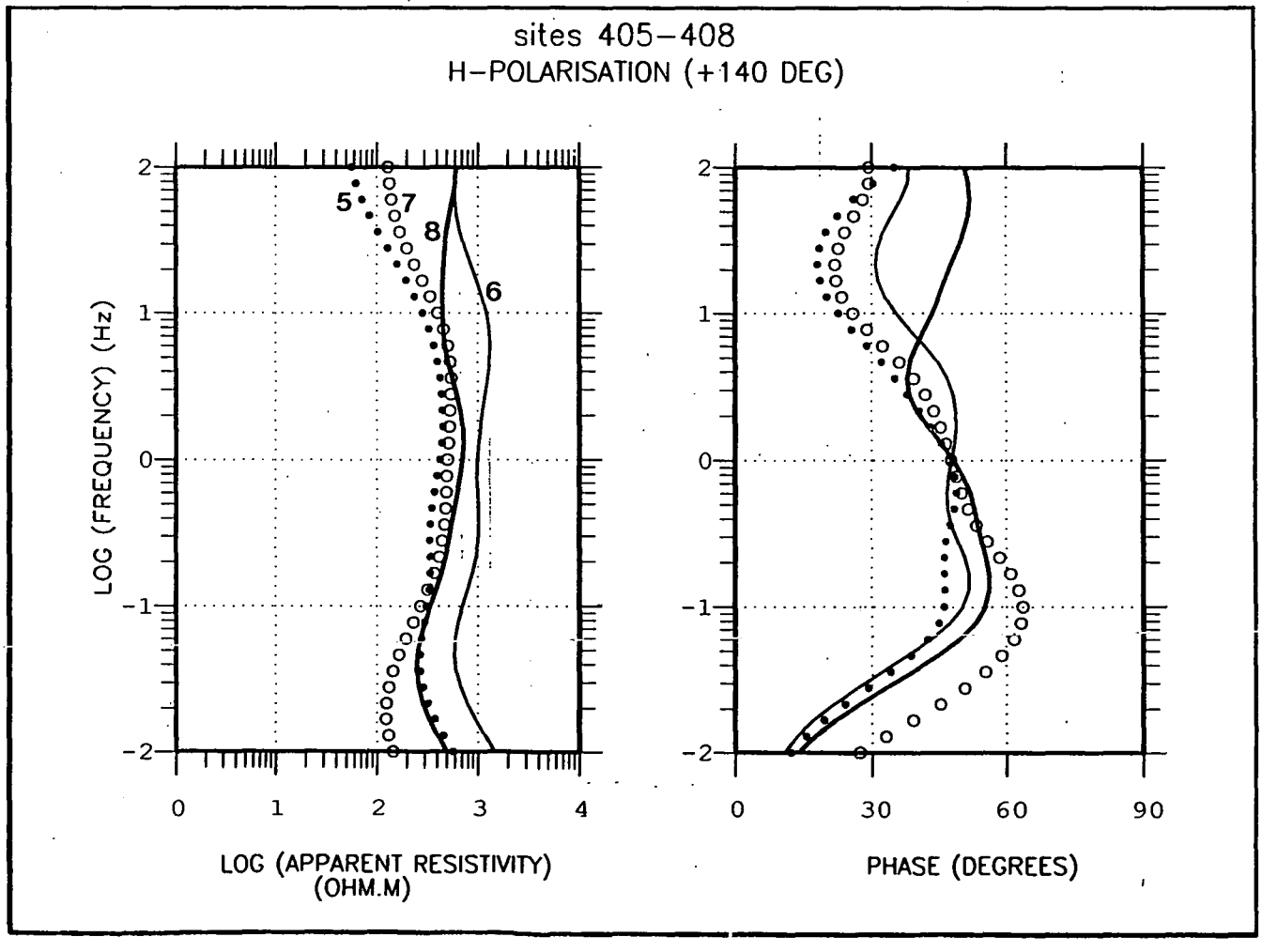
sites 405–408
H–POLARISATION (+140 DEG)
LOG (FREQUENCY) (Hz)
5
7
8
6
LOG (APPARENT RESISTIVITY)
(OHM.M)
PHASE (DEGREES)

THORNHILL MT SURVEY (92)

rms = 4.6

2d OCCAM INVERSION

LOG (RESISTIVITY ohm.m)

V.E. x 0.25

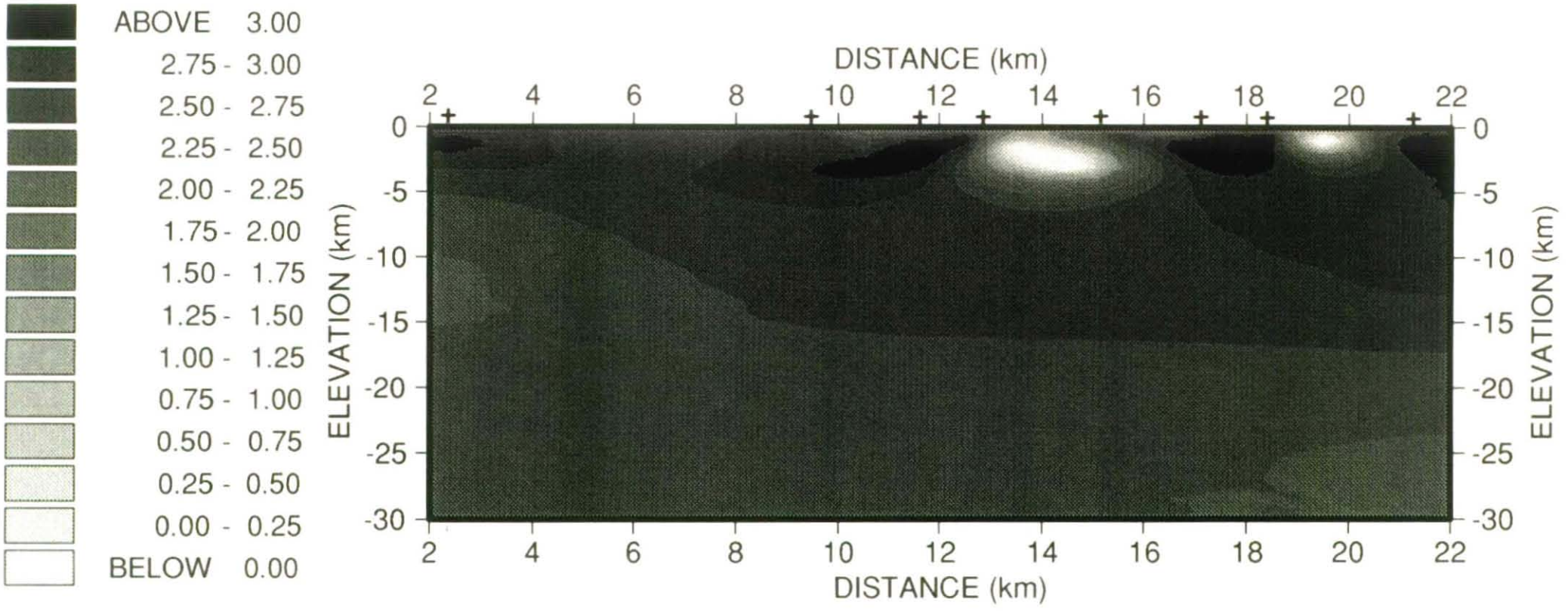

Fig.12

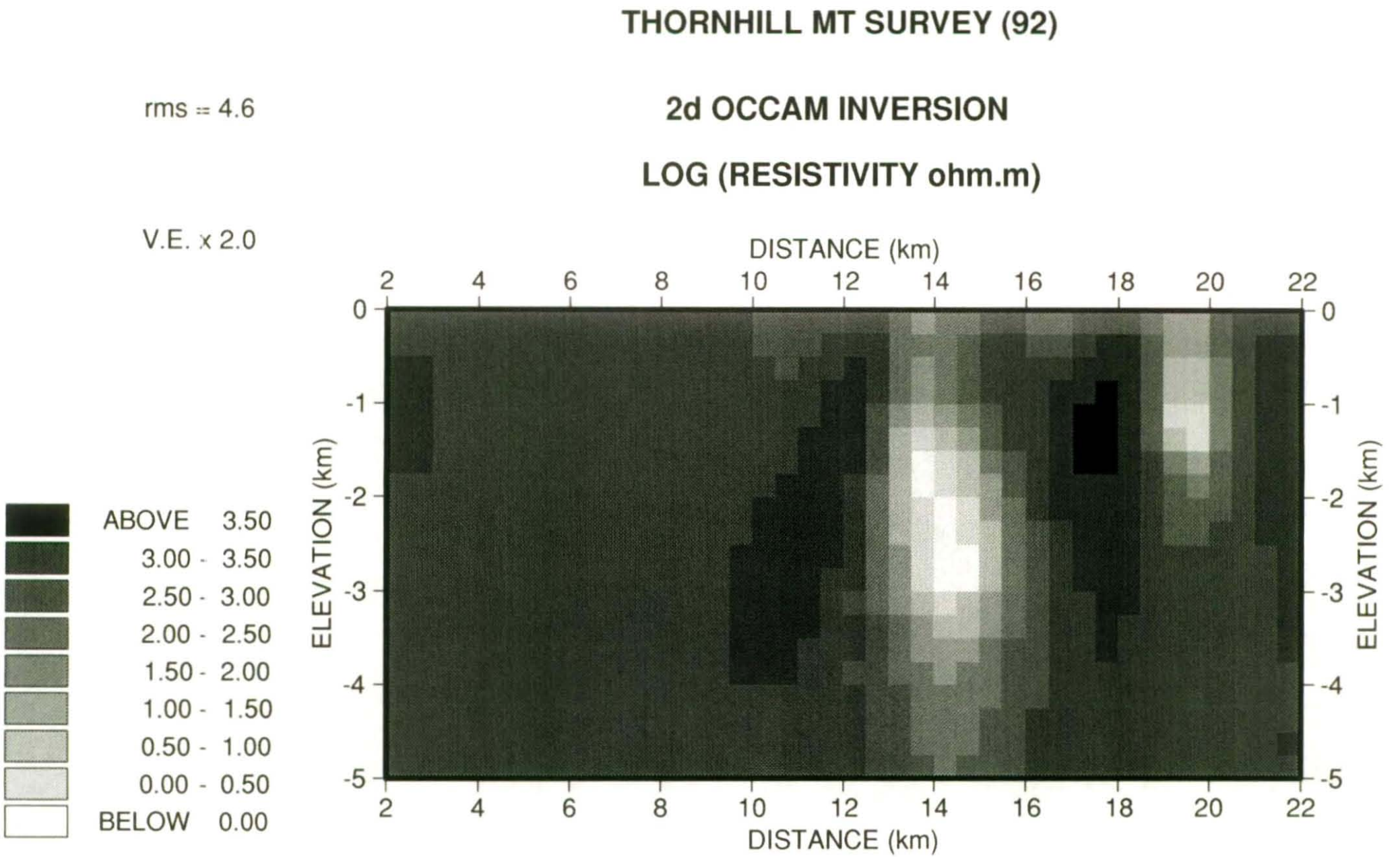
THORNHILL MT SURVEY (92)
rms = 4.6
2d OCCAM INVERSION
LOG (RESISTIVITY ohm.m)
V.E. x 2.0
DISTANCE (km)
2 4 6 8 10 12 14 16 18 20 22
0 -1 -2 -3 -4 -5
ELEVATION (km)
ABOVE 3.50
3.00 - 3.50
2.50 - 3.00
2.00 - 2.50
1.50 - 2.00
1.00 - 1.50
0.50 - 1.00
0.00 - 0.50
BELOW 0.00

Fig.13

S.S. option

rms = 3.0

V.E. x 2.0

THORNHILL MT SURVEY (92)

2d OCCAM INVERSION

LOG (RESISTIVITY ohm.m)

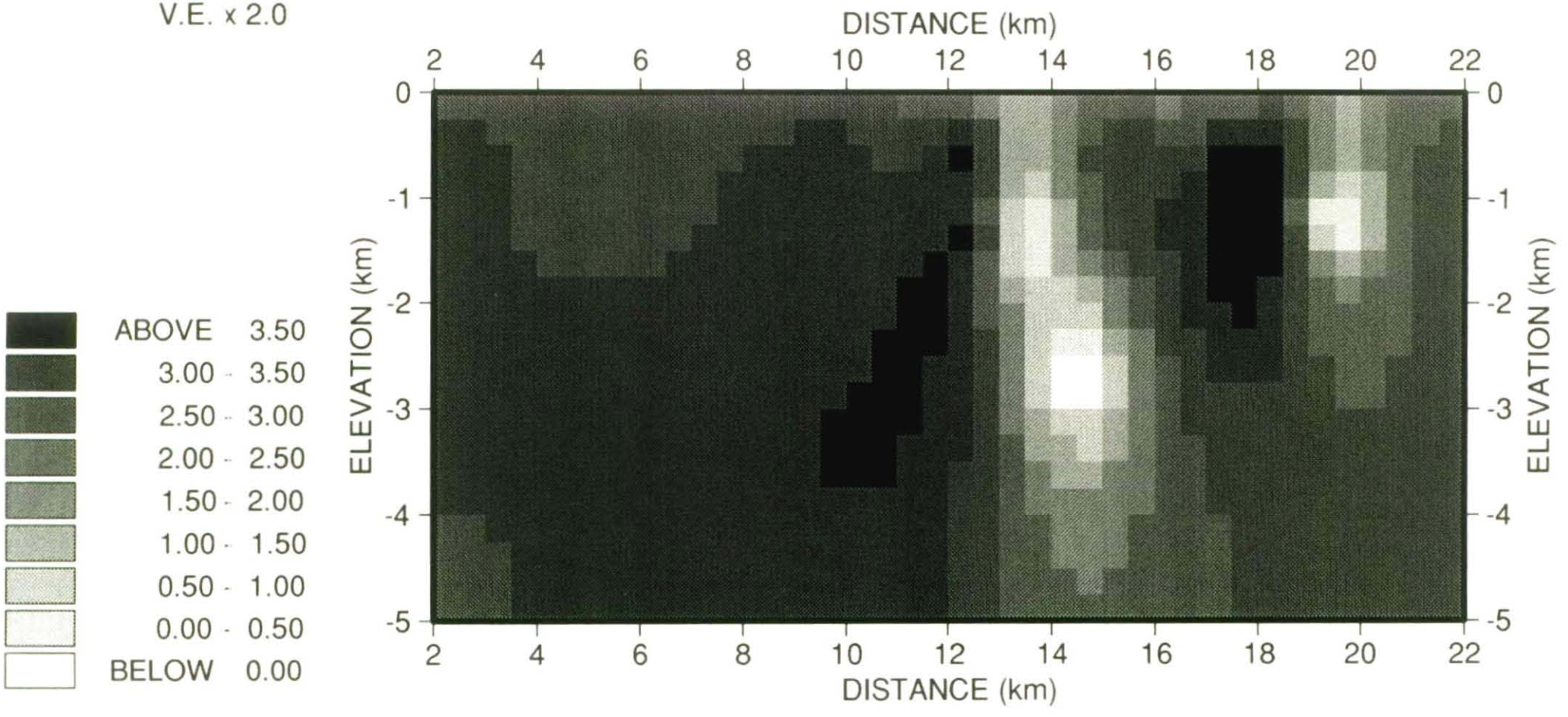

Fig.14

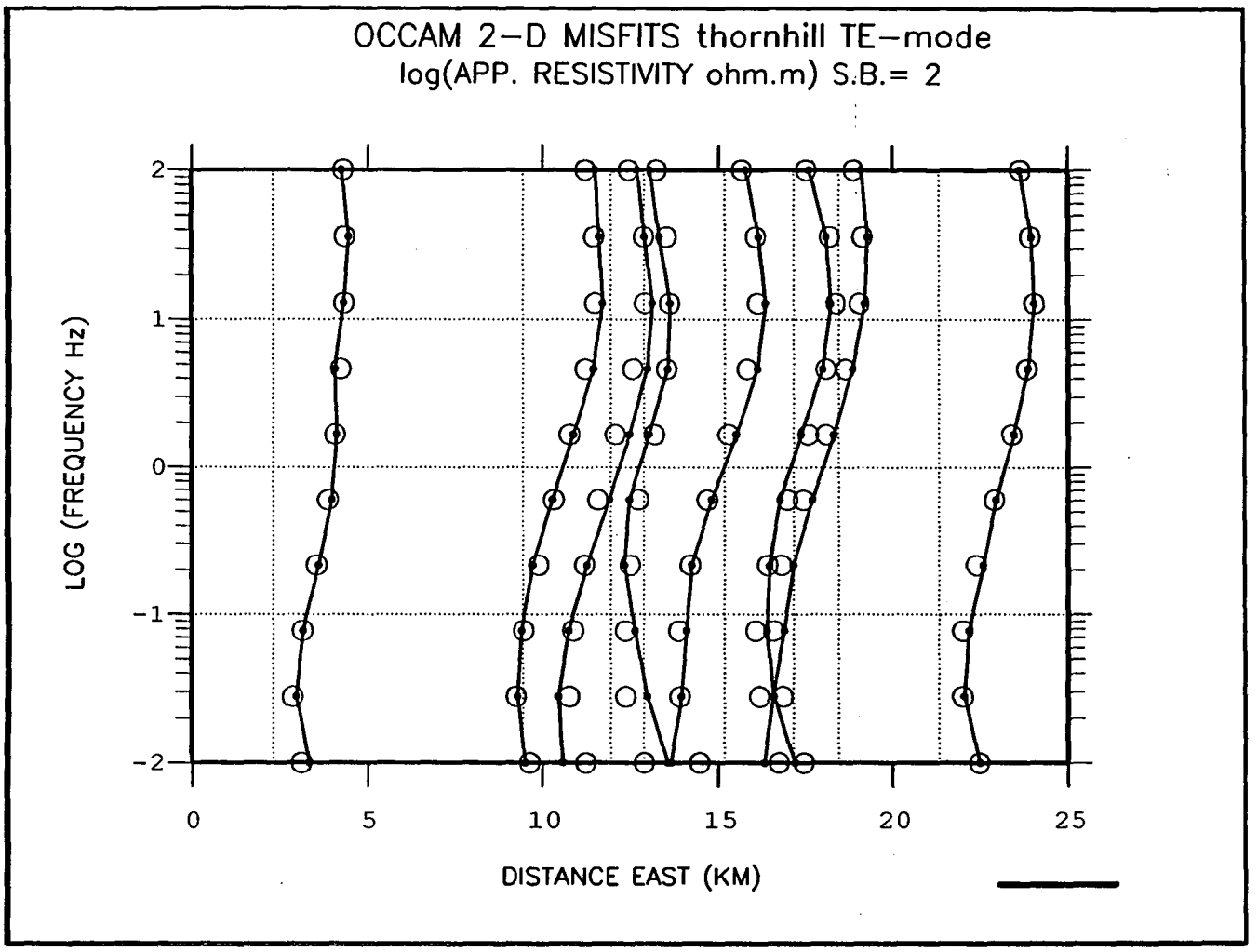
OCCAM 2-D MISFITS thornhill TE-mode
log(APP. RESISTIVITY ohm.m) S.B.= 2
LOG (FREQUENCY Hz)
2
1
0
-1
-2
0
5
10
15
20
25
DISTANCE EAST (KM)

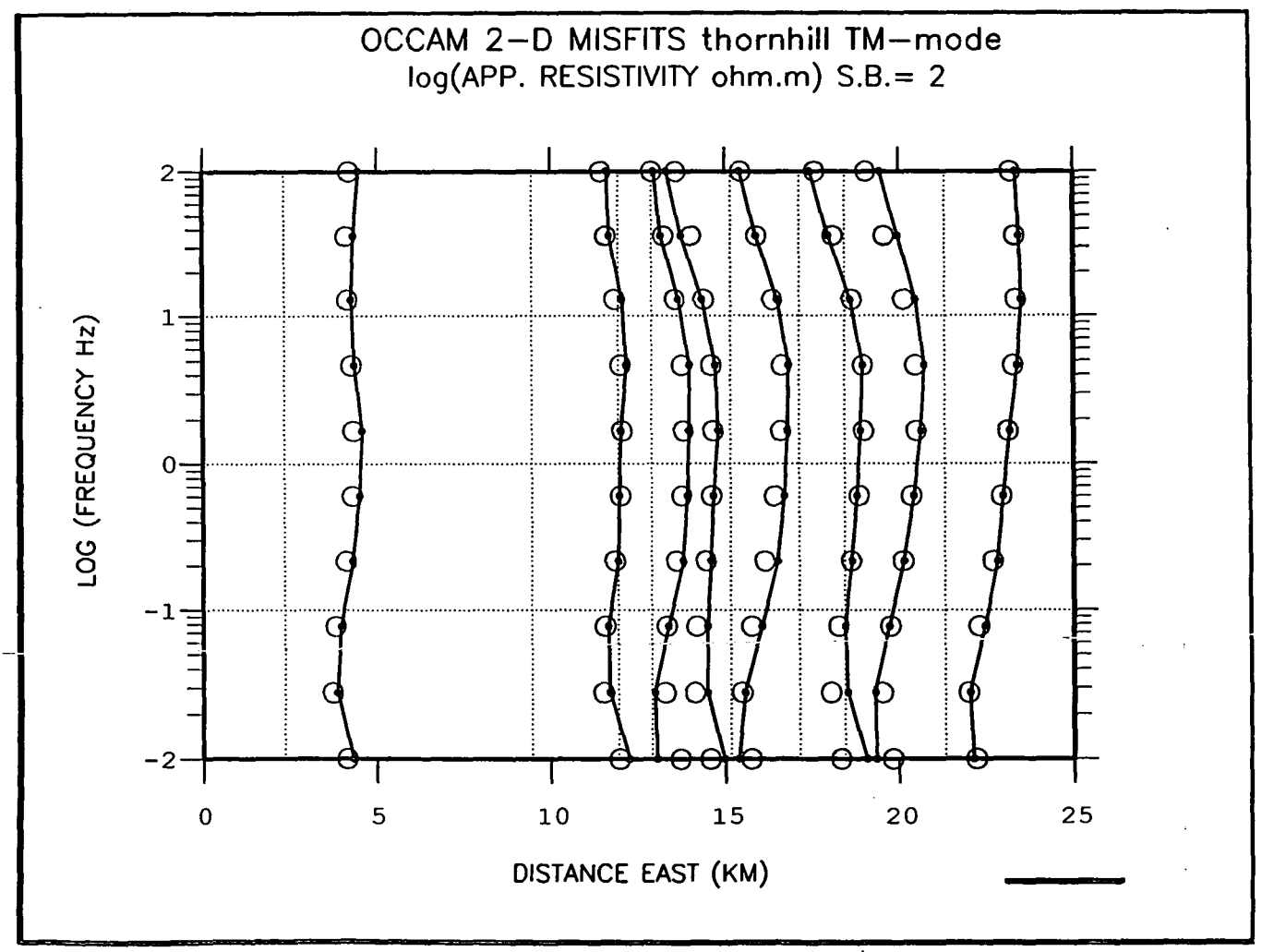
OCCAM 2-D MISFITS thornhill TM-mode
log(APP. RESISTIVITY ohm.m) S.B.= 2
LOG (FREQUENCY Hz)
2
1
0
-1
-2
0
5
10
15
20
25
DISTANCE EAST (KM)

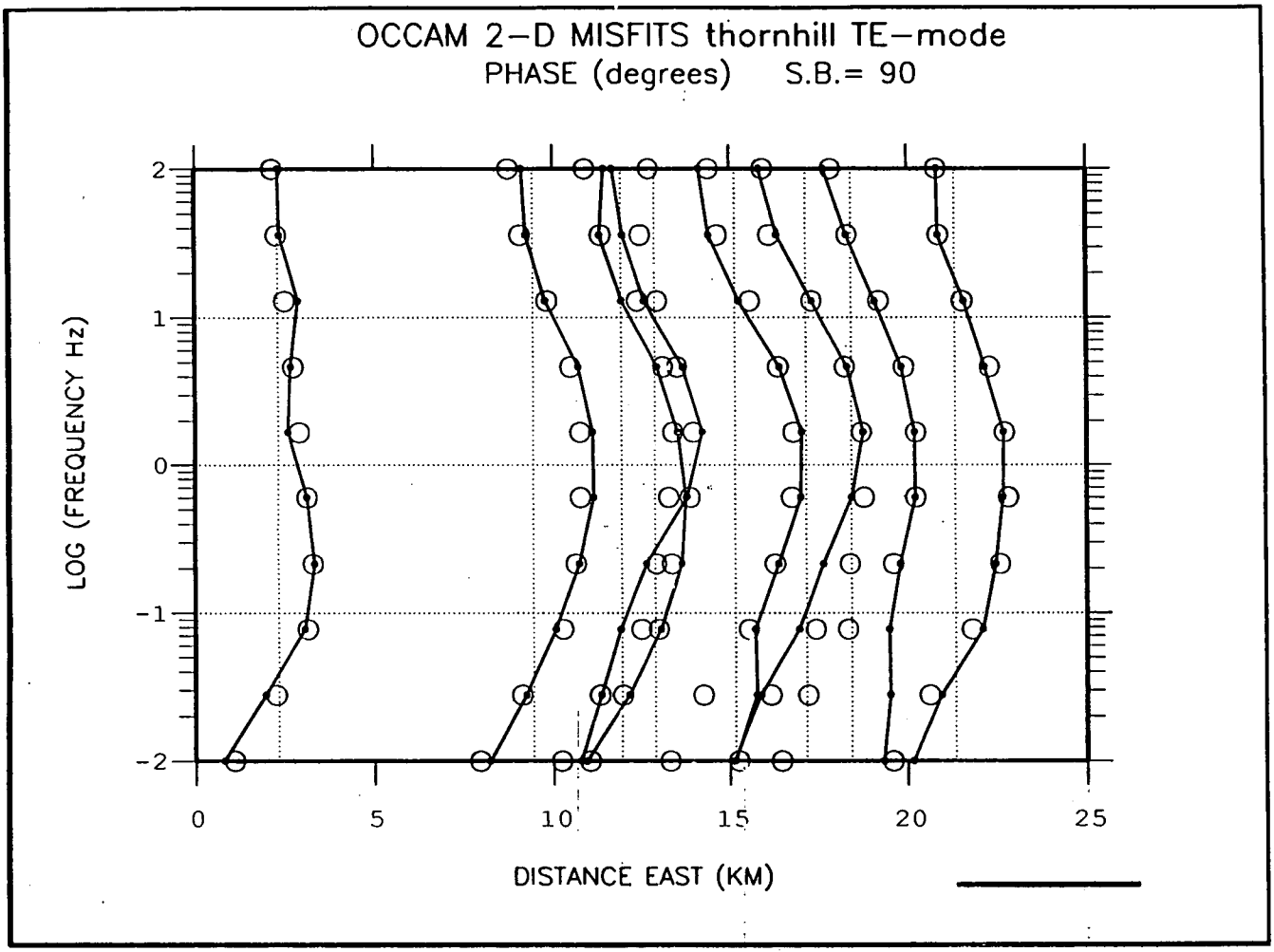
OCCAM 2-D MISFITS thornhill TE-mode
PHASE (degrees) S.B.= 90
LOG (FREQUENCY Hz)
2
1
0
-1
-2
0
5
10
15
20
25
DISTANCE EAST (KM)

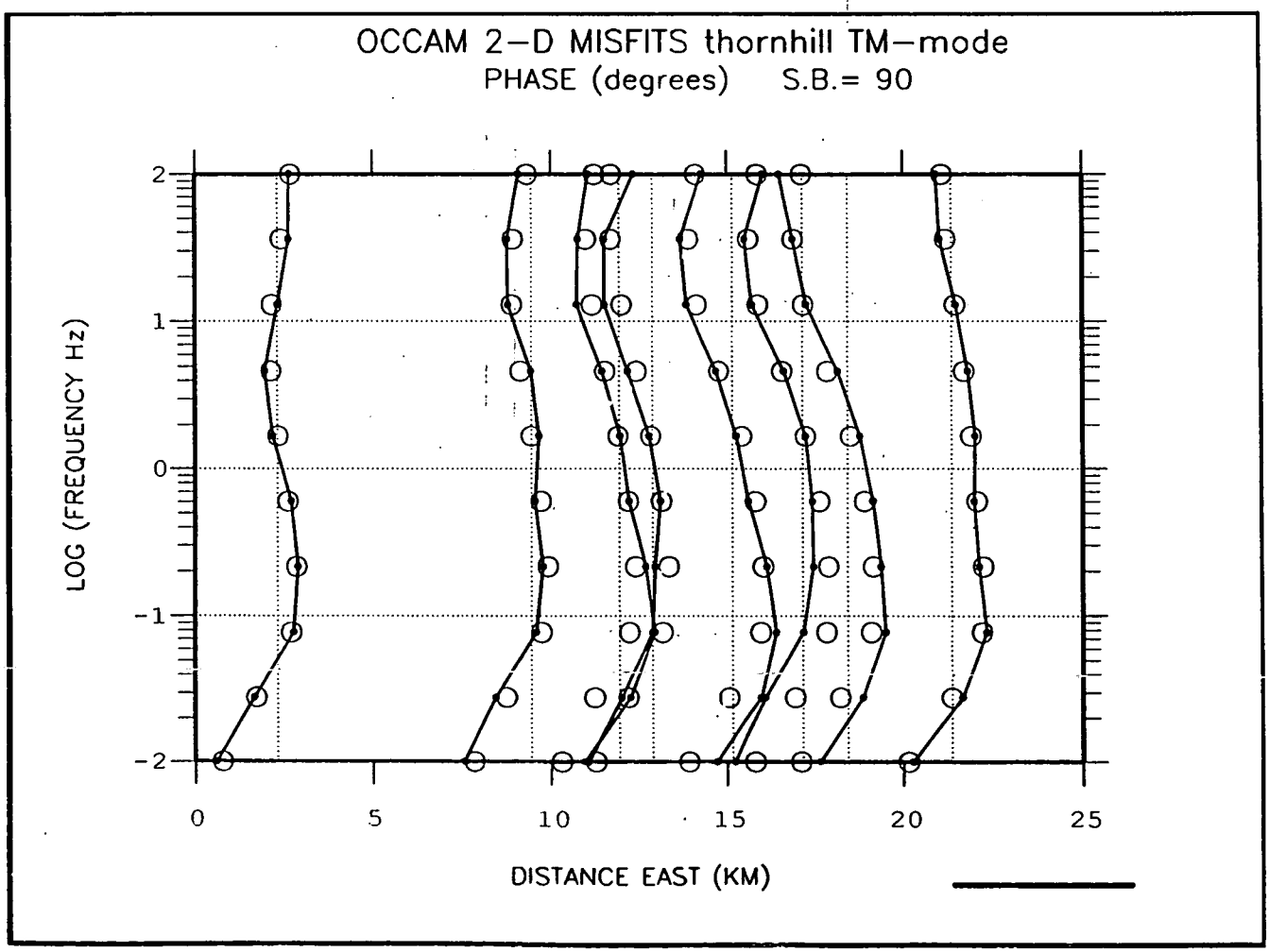
OCCAM 2-D MISFITS thornhill TM-mode
PHASE (degrees) S.B.= 90
LOG (FREQUENCY Hz)
2
1
0
-1
-2
0
5
10
15
20
25
DISTANCE EAST (KM)

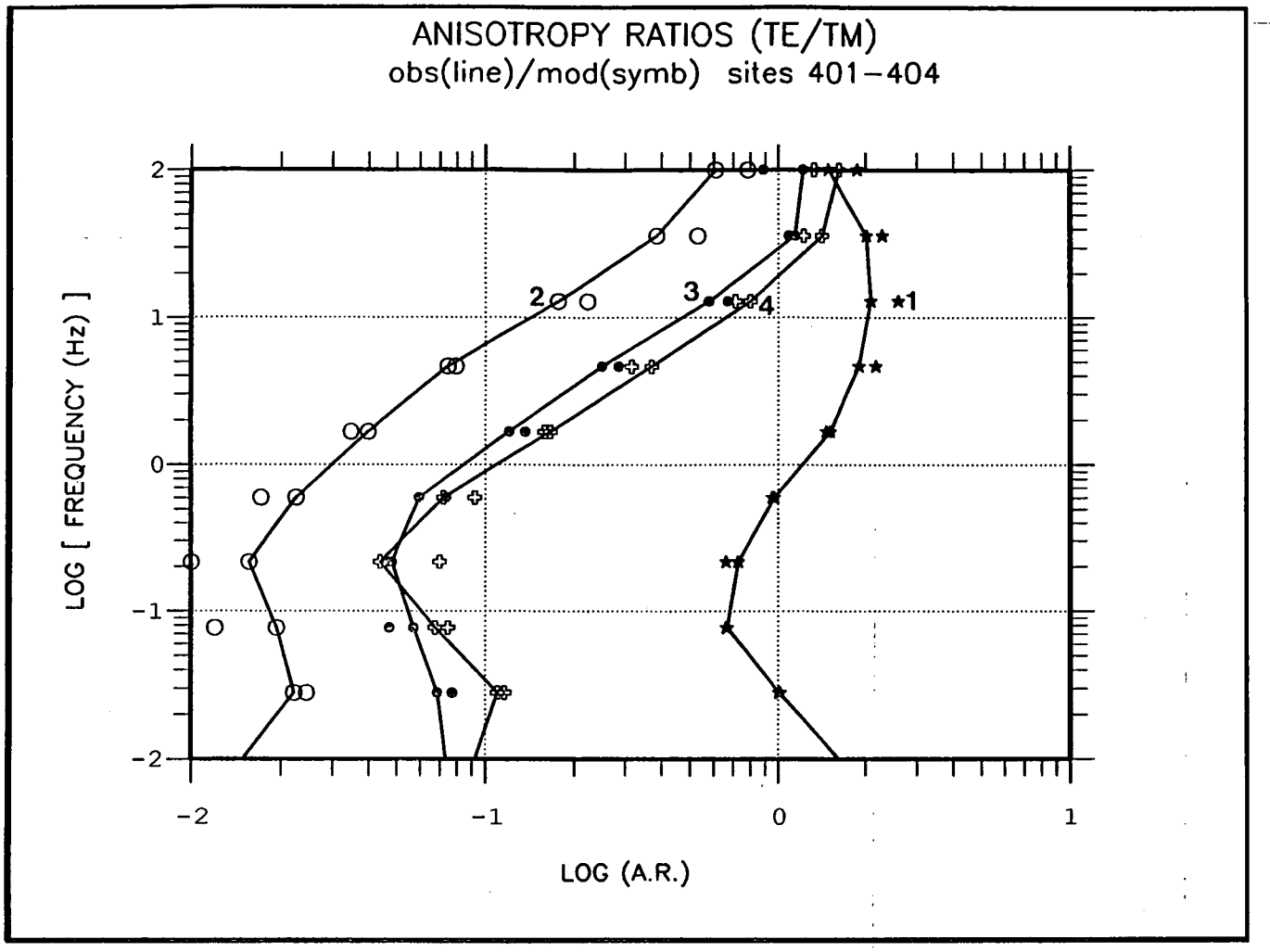
ANISOTROPY RATIOS (TE/TM)
obs(line)/mod(symb) sites 401–404
LOG [FREQUENCY (Hz)]
LOG (A.R.)
2
3
4
1
2
1
0
-1
-2
-2
-1
0
1

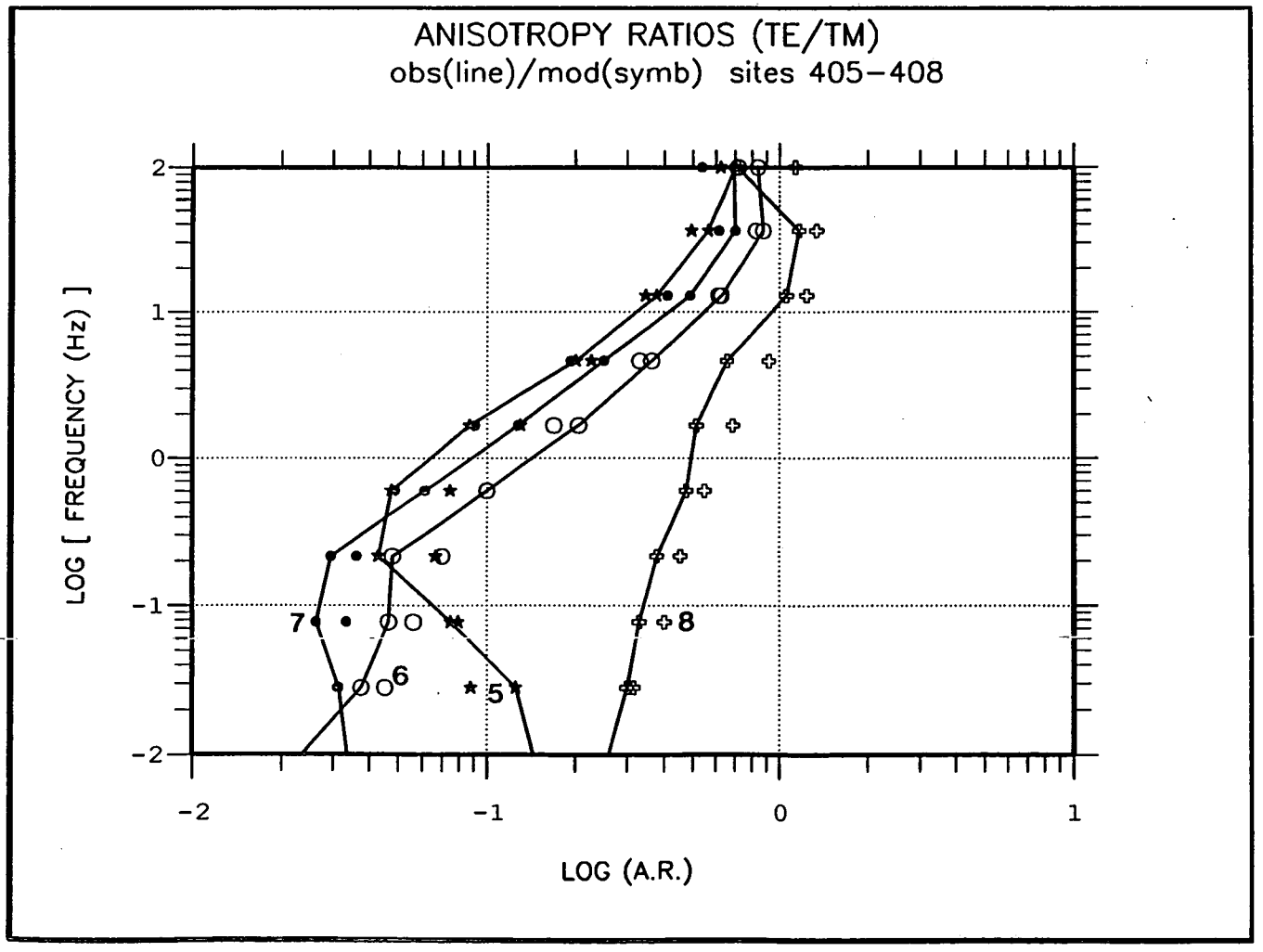
ANISOTROPY RATIOS (TE/TM)
obs(line)/mod(symb) sites 405–408
LOG [FREQUENCY (Hz)]
LOG (A.R.)
7
6
5
8
2
1
0
-1
-2
-2
-1
0
1

THORNHILL MT SURVEY (92)

2d OCCAM INVERSION

rms=4.63

LOG (RESISTIVITY ohm.m)

TRUE SCALE

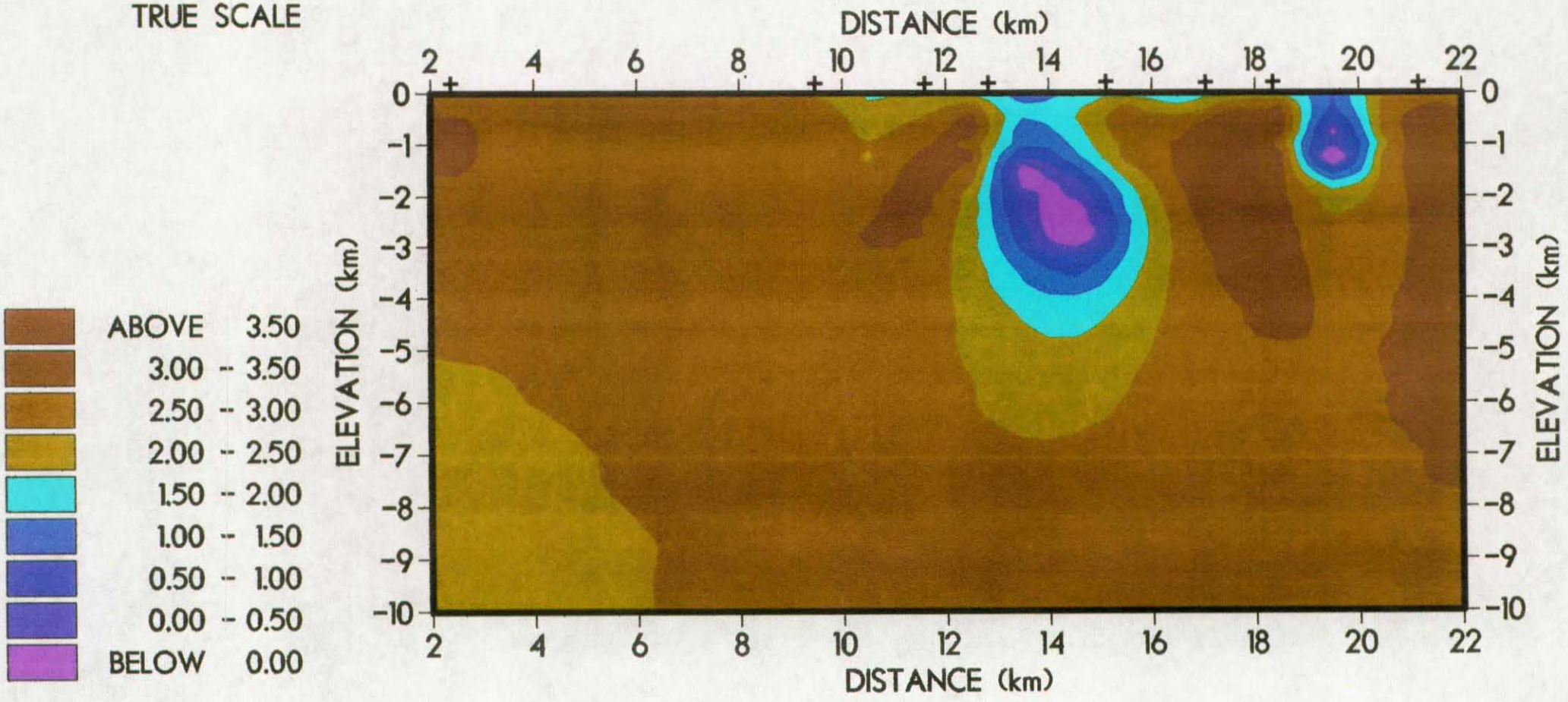

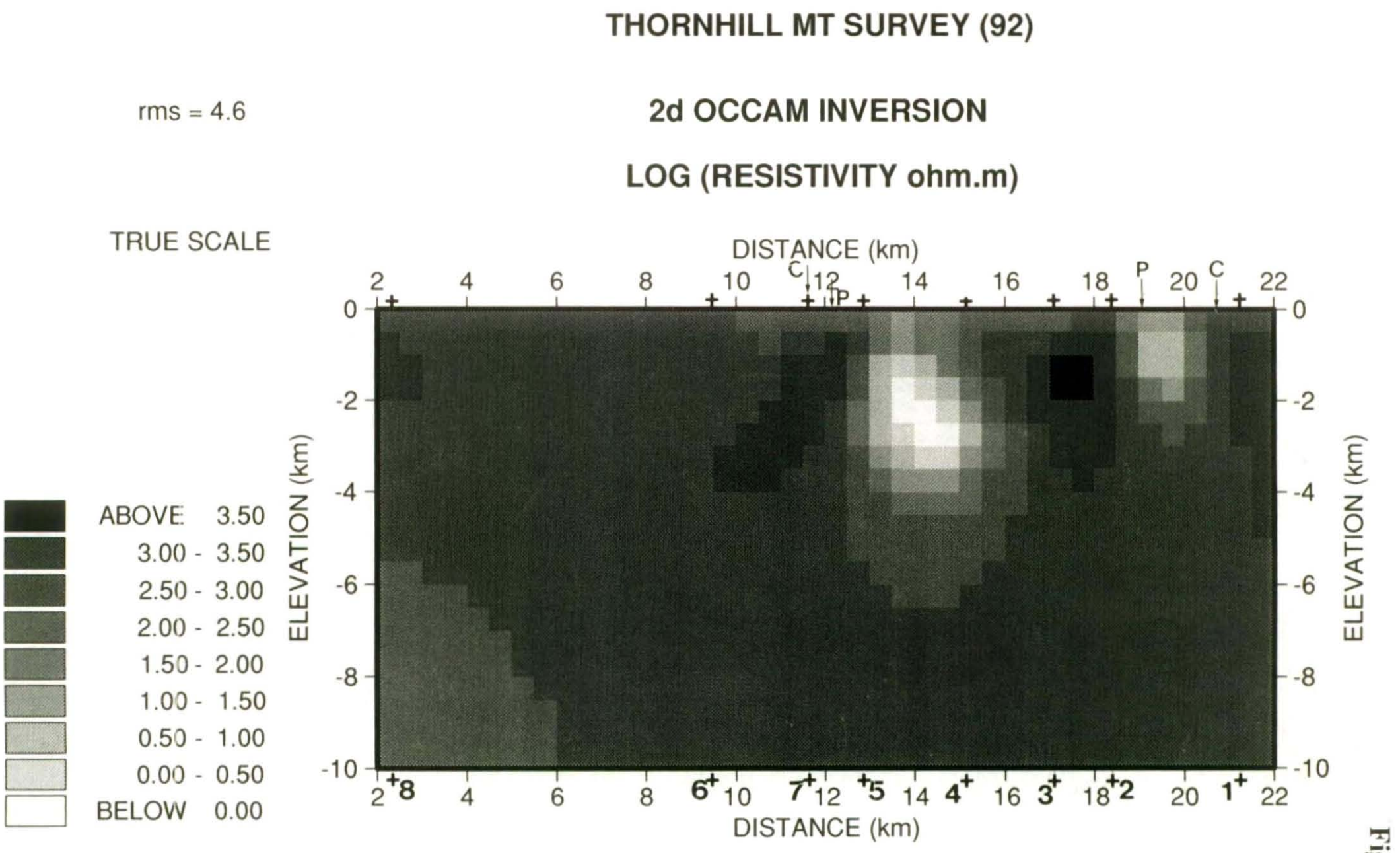
THORNHILL MT SURVEY (92)
rms = 4.6
2d OCCAM INVERSION
LOG (RESISTIVITY ohm.m)
TRUE SCALE
DISTANCE (km)
ELEVATION (km)
ABOVE 3.50
3.00 - 3.50
2.50 - 3.00
2.00 - 2.50
1.50 - 2.00
1.00 - 1.50
0.50 - 1.00
0.00 - 0.50
BELOW 0.00
C
P
8
6
7
5
4
3
2
1

Fig.19